This is A Tribute To The Best TN of All Time

Hogan, Matthew[1] and Toki, Walter[1]

April 19, 2019

[1]Colorado State University, Fort Collins, USA

Abstract

This is the abstract

Contents

List of Figures

List of Tables

1   Introduction

The primary goal of an oscillation experiment is to measure the parameters in a neutrino mixing matrix. All other parameters, with some having some theoretical importance to fundamental physics, are nuisance parameters. To understand the methodology of Beam and Near detector Flux task Force (BANFF) fit, it is relevant to understand how likelihood fitting works.

1.1   Curve Fitting

Curve fitting is commonly found in the particle physics community literature due to the need to compare two models or constrain unknown model parameters using one or more histograms. For the first case, this involves two competing models, H_0 and H_1, in order to establish if the data supports new Physics (H_1) not predicted in the Standard Model (H_0). The second case finds the "best" set of the model predictions, θ, that match the data as is the case for the BANFF fit. In both cases, chi-squared (χ^2) tests are performed to provide goodness of fit, parameter estimation (also referred to as "best fit parameters"), and error/confidence estimation. The chi-squared statistic is derived from a likelihood ratio which asymptotically approaches the classical chi-square distribution. Wilks' theorem guarantees for large data samples that -2 times the logarithm of the likelihood ratio approaches a chi-square distribution.

1.1.1

1.2   ND280

The T2K near detector (ND) complex consists of on-axis and off-axis detectors at 280m away from the secondary beamline proton target. The off-axis detector is used in this analysis which consists of several subdetectors housed inside the UA1/NOMAD magnet yoke as
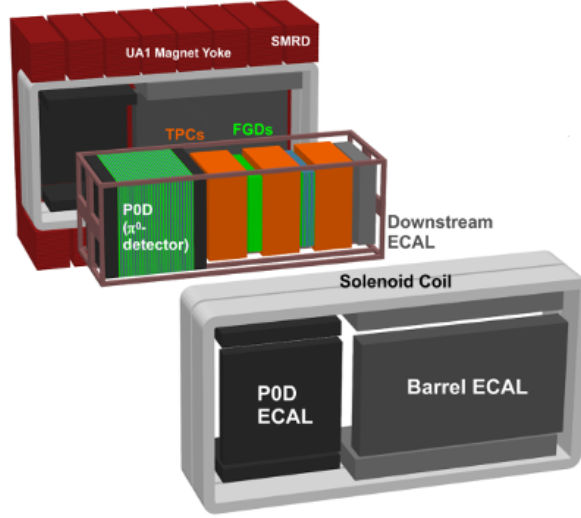
Figure 1.1: Exploded view of the off-axis detectors of ND280. The neutrino beam is directed from left to right along the figure.

shown in figure 1.1. A similar analysis was also performed with the on-axis detector and is available in T2K-TN-335[10]. . The magnet provides a 0.2T magnetic field which is designed to provide momentum and particle identification for the tracker region.

1.2.1   The PØD

The PØD, short for π^0 Detector, is a plastic scintillator based tracking calorimeter inside the ND280 basket. The PØD is constructed as many sandwiches of active and inactive materials designed to fully contain π^0 decay photons. The four primary regions inside the PØD in order of upstream to downstream of the neutrino beam are the upstream ECal (USECal), upstream water target (WT), central WT, and central ECal (CECal). A representation of the entire PØD can be seen in Figure 1.2. Each active module, also called a PØDule, consists of two orthogonally oriented sheets of triangular, scintillator-doped plastic bars as shown in
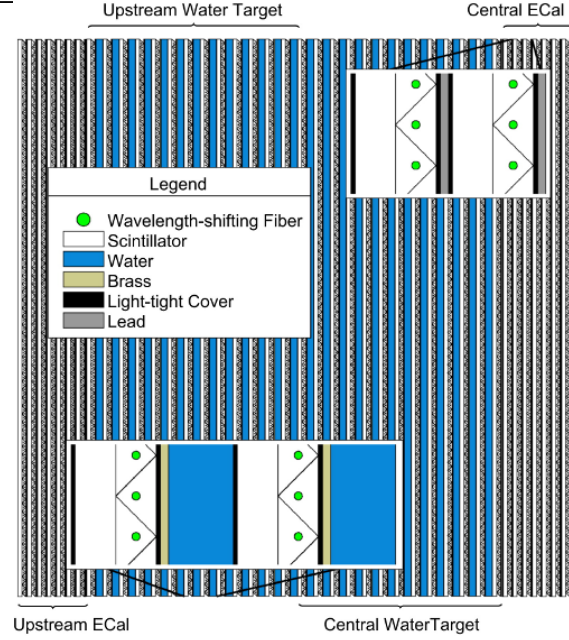
Figure 1.2: This cartoon illustrates the concept design of the PØD where the neutrino beam is approaching from the left.
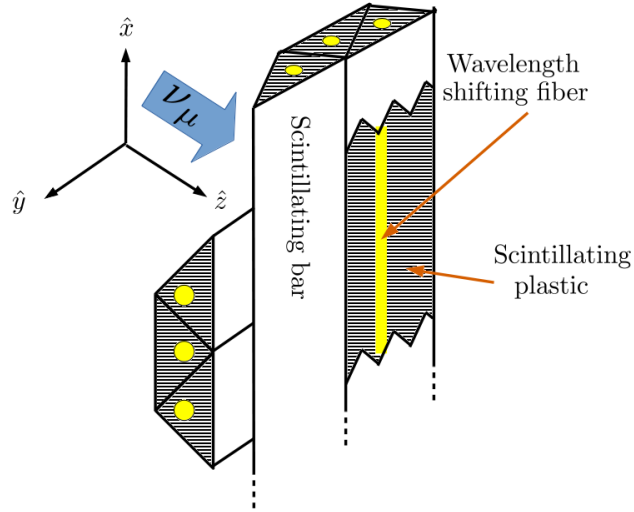
Figure 1.3: This cartoon illustrates the design of a PØDule with orthogonal layers of scintillating, triangular bars. When a charged particle travels through the bar such as a muon from CC interaction, the scintillation light is captured and wavelength shifted inside a fiber bored in the center of each bar. The wavelength shifted light is later observed by a photon counter.

Figure 1.3. The ECal regions are designed to contain decay photons inside the PØD by alternating the scintillator planes with lead sheets. The WT regions, as compared to the lead sheets in the ECals, alternate a thin brass sheet and water filled bags between the PØDules. A unique feature of the PØD is that the water can be drained out resulting in two detector configurations: water-in and water-out.

1.3   Usage of ND280 Psyche Software

Psyche is a general framework for data handling, event selections, and systematic evaluations with toy experiments. Psyche is a "lean" package from the perspective of analyzing MC events since that functionality is built heavily into Highland2. The analysis performed in this technical note required making additions to psyche in order replicate features available in Highland2. It would be wise for future analyses to build a selection in Highland2 and migrate that psyche once mature.

BANFF uses a psyche package called psycheSteering that interfaces with all the psyche tools to manage the migration of samples into its analysis code. New PØD selections were added to the psycheSelections package and validated using the psycheSteering AnalysisManager class. The AnalysisManager provides the functionality to get the true and reconstructed detector observables from each reconstructed event along with the flux tunning and detector systematic weights.

Flux tunning is the process of applying an event weight based on the true neutrino energy, flavor, and run period. Since the ND280 MC uses a series of models to describe the expected neutrino flux, it cannot perfectly model the true flux nor know the beam conditions at run time. The beam group is responsible for releasing the expected and measured neutrino flux in order to account for these differences. To flux tune an event, the relevant neutrino flavor flux histogram must be referenced. The weight is extracted by taking the ratio of the tuned flux to the nominal flux in the MC for a given neutrino energy. As an example Figure 1.4
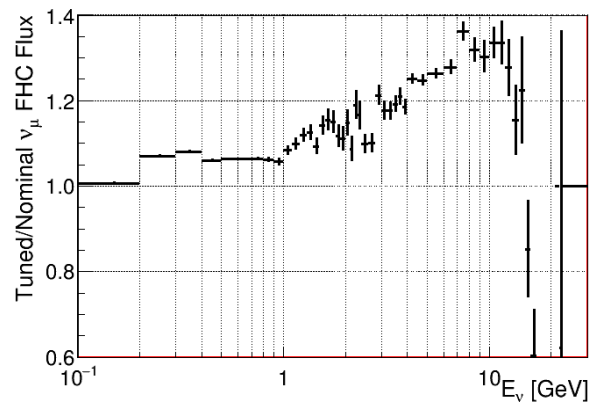
Figure 1.4: Fluxing tuning histogram for ν_μ FHC events taken from the 13av3 flux release.

shows the flux tuning weights for true ν_μ FHC events.

2 BANFF Likelihood

2.1 BANFF Treatment of ND Constraint

The BANFF implementation aims to reduce the dimensionality, and hence complexity, of the joint near detector (ND) and far detector (FD) problem by performing a separate analysis on the nuisance parameters that only the ND can measure. In a joint ND and FD joint fit, the measurements from both detectors are considered along with their respective systematic uncertainties. This approach is computationally expensive since the time to perform a fit increases non-linearly with dimensionality. BANFF considers a ND-only fit in order to decrease the computational demands. The BANFF post-fit parameters and their covariances are then propagated to the oscillation analysis using FD-only data. This allows for more rapidly completed studies on the effects of model parameters and biases present. Conceptually this approach should provide the same result with a joint ND and FD analysis. However, information encoded in the ND measurements for shared nuisance parameters is inevitably lost in this "divide-and-conquer" approach.

The BANFF ND-only constraint between 2015 through 2018 is described in detail in T2K-TN-220[8]. While subsequent updates to the BANFF analysis increase the sample sizes and systematic parameterizations, the method has remained unchanged. It uses a frequentist approach to find the best nuisance parameter set to maximize a binned likelihood.

2.1.1 Constructing a Likelihood

We can define a binned likelihood for the ND280-only constraint with the nuisance parameters. Consider the problem of extracting physics parameters $\vec{y}$ given some data. The

probability to measure these parameters given the data is given as

$$\mathcal{P}\left(\vec{y}\,\middle|\,\vec{N}_{\text{ND280}}^{\text{Data}}\right) = \frac{\mathcal{L}\left(\vec{N}_{\text{ND280}}^{\text{Data}}\,\middle|\,\vec{y}\right)}{\mathcal{P}\left(\vec{N}_{\text{ND280}}^{\text{Data}}\right)}\pi\left(\vec{y}\right),\tag{2.1}$$

where $\vec{N}_{\text{ND280}}^{\text{Data}}$ are the binned data measurements, $\mathcal{P}\left(\vec{N}_{\text{ND280}}^{\text{Data}}\right)$ is a constant normalization, and $\pi(y)$ are prior terms. We have used Bayes' theorem

$$\mathcal{P}\left(AB\right) = \mathcal{P}\left(B\right)\mathcal{P}\left(A\,\middle|\,B\right)\tag{2.2}$$

to evaluate (2.1) as

$$\mathcal{P}\left(\underbrace{\vec{y}}_{A}\,\middle|\,\underbrace{\vec{N}_{\text{ND280}}^{\text{Data}}}_{B}\right) = \frac{\mathcal{P}\left(\vec{N}_{\text{ND280}}^{\text{Data}},\vec{y}\right)}{\mathcal{P}\left(\vec{N}_{\text{ND280}}^{\text{Data}}\right)}\tag{2.3}$$

which we can further manipulate since the data are independent of the nuisance parameters

$$\mathcal{P}\left(\vec{N}_{\text{ND280}}^{\text{Data}},\vec{y}\right) = \mathcal{P}\left(\underbrace{\vec{y}}_{A},\underbrace{\vec{N}_{\text{ND280}}^{\text{Data}}}_{B}\right) = \mathcal{L}\left(\vec{N}_{\text{ND280}}^{\text{Data}}\,\middle|\,\vec{y}\right)\pi\left(\vec{y}\right)\tag{2.4}$$

resulting in the original expression Equation (2.1).

2.1.2 BANFF Likelihood and Test Statistic

Given the likelihood, one desires to find maximal agreement between the predicted and measured data points. For an introduction into the use of likelihood functions in fits to histograms, see [1] and the PDG review on Statistics. Consider many binned samples that select different charged current topologies. A convenient choice of observables for all the samples are the outgoing charged lepton l momentum P_l and angle $\cos\theta_l$ as measured in the ND. Much of this is also documented in T2K-TN-220[8] where additional details can be

found. For each $(P_l, \cos\theta_l)$ analysis bin $i = 1, 2, \ldots, M-1, M$, the likelihood $\mathcal{L}$ is given by

$$\mathcal{L}\left(\vec{N}^p \,\middle|\, \vec{N}^d\right) = \left(\prod_{i=1}^{M} \left(\vec{N}_i^p\right)^{\vec{N}_i^d} \frac{e^{-\vec{N}_i^p}}{\vec{N}_i^d!}\right) \tag{2.5}$$

where $\vec{N}^d$ is the number of observed data events and $\vec{N}^p$ is the number of predicted events as a function of many nuisance parameters. One recognizes the likelihood function as a Poisson distribution given this is a counting experiment. The sets of dependent nuisance, also called systematic, parameters that affect the predicted event rate are

- cross section (xsec) physics model parameters,

- neutrino flux, and

- detector systematics.

Given these three sets of systematics, the number of predicted events is given by

$$\vec{N}_i^p\left(\vec{x}, \vec{b}, \vec{r}\right) = w_i^{\mathrm{POT}} \vec{d_i} \sum_{j=1}^{N_i^{\mathrm{MC}}} \left[\sum_{k=1}^{N^{\mathrm{Flux}}} \left(\delta_{j,k}^{\mathrm{Flux}} \vec{b}_k\right) \prod_{l=1}^{N^{\mathrm{Syst}}} w_{j,l}\left(\vec{x}_l^{\mathrm{xsec}}\right)\right]. \tag{2.6}$$

Here w_i^{POT} is the the ratio of of the number of true to simulated (MC) protons on target (POT) and N_i^{MC} is the number of events in the ith analysis bin. The $\vec{d_i}$ parameters are observable normalization detector systematic parameters that vary the total number of predicted events in the analysis bin. The $\vec{b}_k$ parameters, out of a total of N^{Flux}, are flux normalization systematics for each flux bin. Since the flux bins are categorized by neutrino flavor, energy, and horn (focusing magnet) current, the $\delta_{j,k}^{\mathrm{Flux}}$ term selects the correct flux bin. The $w_{j,l}\left(\vec{x}_l^{\mathrm{xsec}}\right)$ parameters are pre-calculated event weight functions for each cross section (xsec) model parameter, $\vec{x}_l^{\mathrm{xsec}}$, out of a total of N^{Syst} cross section systematics.

In practice one tries to minimization a test statistic which programs like MINUIT are designed to find. Using the likelihood ratio test theorem, a test statistic can be defined using

a ratio of two likelihoods

$$\Delta\chi^2_{\text{ND280}} = -2\log\frac{\mathcal{L}\left(\vec{N}^p \middle| \vec{N}^d\right)}{\mathcal{L}\left(\vec{N}^d\right)} \tag{2.7}$$

where this test statistic $\Delta\chi^2_{\text{ND280}}$ obeys a true chi-squared distribution for asymptotically large statistics. Penalty terms from the cross section, flux, and detector systematics are included in order to account for their systematic effect. The updated test statistic is given by

$$
\begin{aligned}
\Delta\chi^2_{\text{ND280}} = {} & -2\log\frac{\mathcal{L}\left(\vec{N}^p \middle| \vec{N}^d\right)}{\mathcal{L}\left(\vec{N}^d\right)} + \Delta\chi^2_{\text{xsec}} + \Delta\chi^2_{\text{Flux}} + \Delta\chi^2_{\text{Det}} \\
& -2\log\frac{\mathcal{L}\left(\vec{N}^p \middle| \vec{N}^d\right)}{\mathcal{L}\left(\vec{N}^d\right)} - 2\left(\sum_{\vec{y}=\vec{x},\vec{b},\vec{r}} \log\left[\frac{\pi\left(\vec{y}\right)}{\pi\left(\vec{y}_{\text{Nom}}\right)}\right]\right)
\end{aligned}
\tag{2.8}
$$

with each of the prior distributions $\pi\left(\vec{y} = \vec{x}, \vec{b}, \vec{d}\right)$ assumed as normally distributed priors

$$\pi(\vec{y}) = \left(\frac{1}{(2\pi)^{k_y}\det\left(V_y\right)}\right)^{\frac{1}{2}} e^{\left(-\frac{1}{2}\Delta\vec{y}\cdot V_y^{-1}\cdot\Delta\vec{y}^T\right)}, \tag{2.9}$$

with V_y being the covariance matrix for a k_y size vector $\vec{y}$, $\Delta\vec{y} = \vec{y} - \vec{y}_{\text{Nom}}$ is the difference between the current/explored and nominal set of vector parameters, and T corresponds to the transpose of a vector. The full expanded form of the test $\Delta\chi^2_{\text{ND280}}$ is given by

$$
\begin{aligned}
\Delta\chi^2_{\text{ND280}} = {} & 2\sum_{i=1}^{M}\left[\vec{N}_i^p - \vec{N}_i^d + \vec{N}_i^d\log\left(\frac{\vec{N}_i^d}{\vec{N}_i^p}\right)\right] \\
& + \Delta\vec{x}\cdot V_x^{-1}\cdot\Delta\vec{x}^T + \Delta\vec{b}\cdot V_b^{-1}\cdot\Delta\vec{b}^T + \Delta\vec{d}\cdot V_d^{-1}\cdot\Delta\vec{d}^T \\
& + \log\left[\det\left(V_x\right)\right] + \log\left[\det\left(V_b\right)\right] + \log\left[\det\left(V_d\right)\right] \\
& + \log\left[\det\left(V_x^{\text{Nom}}\right)\right] + \log\left[\det\left(V_b^{\text{Nom}}\right)\right] + \log\left[\det\left(V_d^{\text{Nom}}\right)\right]
\end{aligned}
\tag{2.10}
$$

What follows here is a further description of the systematics and their implementation.
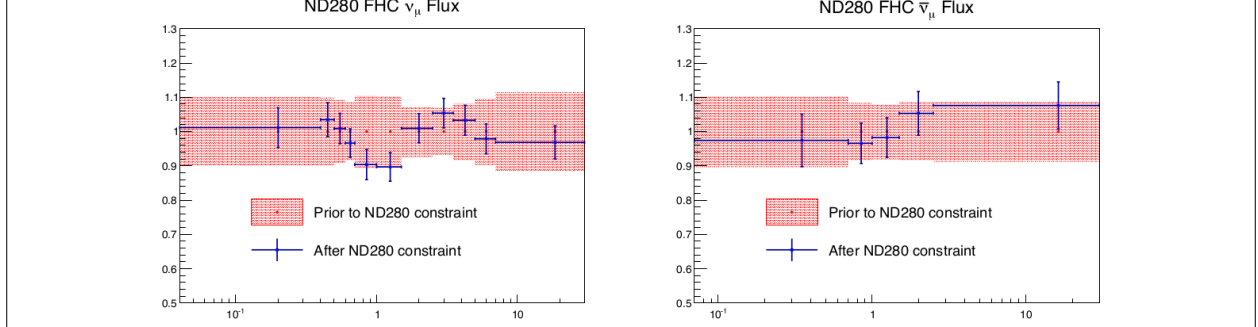
Figure 2.1: BANFF ND280 flux ν_μ and $\overline{\nu}_\mu$ binning parameters from T2K-TN-324 data post-fit results. The uncertainties are extracted from the pre-fit and post-fit covariance matrices.

2.1.3 Flux, Cross Section, and Detector Systematics

The minimization of the LLH is attempted by exploring the multidimensional parameter space to as best as possible match the data and prediction. To understand the response of each systematic, a covariance matrix is built for each source. A combined covariance matrix is used in used the BANFF analysis where each sub-matrix is initially uncorrelated with each other. The parameters in the covariance matrix are usually given a nominal value of one (1) unless a special value is needed with an uncertainty extracted using the Cholesky decomposition method. The development of each systematic uncertainty is briefly discussed below.

Flux: The flux weight is binned as a function of neutrino energy E_ν and divided by horn current (RHC or FHC) and neutrino flavor (ν_μ, $\overline{\nu}_\mu$, ν_e, and $\overline{\nu}_e$). Each flux bin has a preset width with parameter that describes the weight and its uncertainty as shown in Figure 2.1 . Each parameter has a nominal value of one (1) and an increase of 10% (1.1) indicates the corresponding bin increases by 10% also. There are 50 ND and 50 SK parameters with a flux covariance matrix is shown in Figure 2.2 .

Cross Section: There are a number of cross section models and weight functions implemented in BANFF. The cross section model used in this analysis is the 2017 NIWG parameterization. A technical description of the 2017 parameterization is given in T2K-TN-
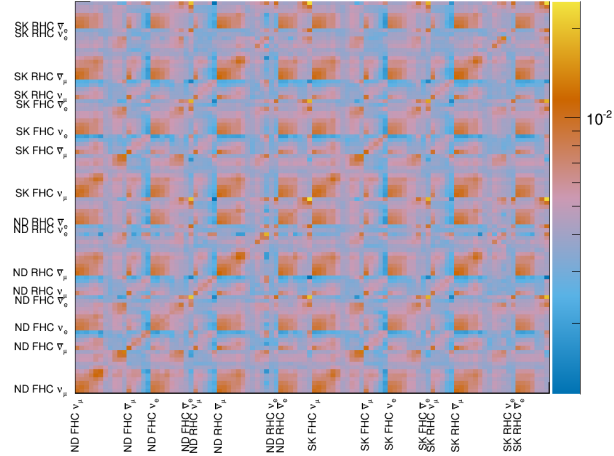
Figure 2.2: BANFF pre-fit flux covariance matrix shown with respective detector, horn current, and neutrino flavor.
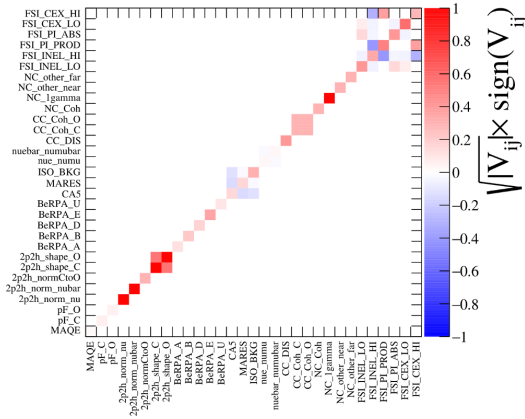
Figure 2.3: Cross section parameters pre-fit correlation matrix from the 2017 BANFF analysis.

315[3] and T2K-TN-307[11]. In general, there are model parameters that describe CC-0π, CC-1π, FSI (FSI: final state interactions, and smaller T2K effects. There are 25 cross section parameters as shown in Figure 2.3 [2].

Detector Systematics: Detector systematics are implemented as normalization changes to event kinematics as well as sample migration. In order to understand the how the detector systematics affect analysis bins, BANFF employs what are called observable normalization parameters, also commonly refered to as obsnorms. Since neutrino interaction events can

migrate from sample-to-sample, bin-to-bin, or both depending on the relevant systematics, numerous toy experiments are performed by varying detector systematic model parameters . After many toy experiments, usually 2000, all the toy experiments are examined together to create a covariance matrix. The drawback to this method is that not all detector systematics have Gaussian responses to the observables, and so the correlations are not fully accurate.

Ideally there would be one observable normalization for each analysis bin. However due to computational and time limitations, a single observable normalization parameter is assigned to multiple analysis bins. The number of observable normalization parameters are determined by the analyzer by merging the sets of analysis bins.

3 PØD Selections and Data Samples

This section describes the development of ν_μ and $\overline{\nu}_\mu$CC-Inclusive selections in both FHC and RHC beam configuration for PØD-based analyses. These selections are the continuation of previous works that developed ν_μ CC-Inclusive selections between the PØD and TPC1. The first such analyses were T2K-TN-80 and T2K-TN-100 which described the ν_μ CC-Inclusive event selection and, later, cross-section analysis using ND280 Production 5 software, respectively[5, 6]. These analyzes relied on each sub-detector's reconstruction software and developed a track matching algorithm since the ND280 "Global" reconstruction matching was problematic in Production 5. As the inter-detector matching reconstruction improved in "Global", two CC-0π cross section analyzes, T2K-TN-258 and T2K-TN-328, were developed that also used the CC-Inclusive selection as pre-selection cuts[13, 4]. The selections described in this technical note also employ the same pre-selection cuts. What follows from here in this section is a layout of the following topic discussions.

The first topic discussed in this section is a description of the π^0 Detector (PØD). The next topic is the event reconstruction using the "Global" reconstruction software. Following that is the pre-selection cut flow. With the pre-selection cuts established, each of the three CC-Inclusive selection's cut flow is described. Concluding this section is a discussion of the three samples in the following order: ν_μ in FHC mode, $\overline{\nu}_\mu$ in RHC, and ν_μ in RHC.

3.1 Global Reconstruction

The task of the Global reconstruction is to combine ND280 sub-detector reconstruction into an single reconstructed object. It was originally designed to analyze "CCQE-like" events in the Tracker region and has been extended with all of ND280. Global attempts to match and re-fit individual sub-detector objects using a Kalman filter while correcting for energy loss and multiscattering. A vertex associated with the re-fit object is also extracted using

19

Run Period	Horn Current	PØD Status	Data POT $\left(\times 10^{20}\right)$	MC POT $\left(\times 10^{20}\right)$
2	+250 kA	Water	0.4339	12.03
		Air	0.3591	9.239
3b	+205 kA		0.2172	4.478
3c	+250 kA		1.364	26.32
4			1.782	34.99
		Water	1.642	34.97
5c	-250 kA		0.4346	22.77
6b		Air	1.288	14.17
6c			0.5058	5.275
6d			0.7753	6.884
6e			0.8479	8.594
7b		Water	2.436	33.70
8	+250 kA		1.580	26.46
		Air	4.148	36.06
Sand	FHC		-	11.19
Sand	RHC		-	12.92
2, 3b, 3c, 4, 8	FHC	Air	7.872	79.18
2, 4, 8		Water	3.657	73.47
6b, 6c, 6d, 6e	RHC	Air	3.417	34.92
5c, 7b		Water	2.871	56.48

Table 3.1: T2K MC and data POT divided by run periods. The bottom four rows are the aggregrated periods grouped by horn current and PØD status which is how the data analysis is performed.

a different Kalman filter. A detailed description of the track matching and vertex finding algorithms for Global is described in T2K-TN-46[12].

3.2 Data Sets

The data sets used in this analysis are runs 2-8 in both PØD water-in and water-out (air) modes as shown in Table 3.1.

3.3 PØD Selection Cuts

The selection of CC-Inclusive events use a series of cuts to select the primary lepton. The pre-selection cuts ("precuts") are applied first to extract events that start in the PØD FV. A MIP is more likely to reach TPC1 from the PØD FV since the PØD is constructed out of heavy materials especially in the CECal. So the main track each selection is designed to select a muon.

This following sections will describe the precuts common to all CC-Inclusive selections and the branching of different cuts, after the precuts, to select the main track.

3.3.1 Pre-Selection Cuts

The pre-selection ("precuts") were initially developed to select ν_μCC-Inclusive using the PØD and TPC sub-detector reconstruction softwares separately[5]. They were then used with the Global reconstruction software for the ν_μCC-0π selection in the FHC beam configuration as described in technical note T2K-TN-258[13]. The description and flow of the precuts are described here as well since there is an incomplete description of the selection precuts.

The precuts are performed on each bunch per beam spill as follows

1. The event has a "good" data quality flag.

   - An event is rejected if any sub-detector or electronics in ND280 reported as "bad" during that bunch.

2. There is at least one (1) track reconstructed in TPC1.

   - There are no restrictions on the number of tracks fully contained in the PØD or exiting into other sub-detectors.

3. The track in TPC1 must have more than 18 nodes.

21

- The TPC reconstruction gathers vertical and horizontal hits into clusters of hits. The charge distribution of the cluster is used to get a vertical (horizontal) position that is more accurate than the individual readout pads. A node is constructed out of each cluster with associated track state information. The set of nodes are used to fit the track helix[9].

4. The reconstructed vertex is within the PØD WT FV.

   - The PØD FV is defined to include as much as the WT regions as possible. Its X and Y borders are 25 cm away from the PØDule edges while its Z borders intersect the last and first half downstream PØDule in the USECal and CECal, respectively. The enumerated volume edges are shown in table 3.2. This volume, while used for track-based analyzes in the past, was optimized for π^0 and ν_e analyzes[7].

5. All tracks that enter TPC1 pass the veto cut

   - An event is rejected if any PØD track enters TPC1 from outside the "corridor" volume. This cut was designed to eliminate broken tracks between the PØD and TPC1 when the separate sub-detector reconstructions were used[5]. In practice, this cut ensures that Global tracks entering TPC1 away from its X and Y edges. The corridor definition is the same as defined in T2K-TN-208 and shown in Table 3.2.

PØD WT FV			Corridor Volume		
-836	< X <	764	-988	< X <	910
-871	< Y <	869	-1020	< Y <	1010
-2969	< Z <	1264	-3139	< Z <	-900

Table 3.2: The PØD WT FV (left) and veto corridor volume (right) in the ND280 coordinate system. The corridor spans from the 5th (8th) to 40th (80th) PØDule (scintillator layer). All the units are given in millimeters.

After passing all the precuts, a single, global track, which is observed in TPC1, is assigned as the "main track" of a selection. The main track for ν_μ selections is the highest momentum, negatively-charged track (HMNT). Similarly the highest momentum, positively-charged track (HMPT) is assigned the main track for $\overline{\nu}_\mu$ selections.

This concludes the application of precuts to all the CC-Inclusive selections. The following subsubsections describe the CC-Inclusive selection cuts, first in FHC mode and then RHC mode.

3.3.2   CC-Inclusive in FHC

As discussed in Section section 3.3.1 on page 21, this selection is the basis for the ν_μ CC-0π PØD+TPC1 analysis. This is FHC mode selection and so the lack of a negatively charged track is the final cut for the CC-Inclusive selection.

3.3.3   CC-Inclusive in RHC

3.4   PØD Water-Out Samples

This section shows the kinematic distributions for the PØD water-out samples. First an examination of the CC-Inclusive samples and the effects of the systematic weights will be explored. The samples are then examined as CC 1-track and CC N-tracks.

3.4.1 CC-Inclusive

The CC-Inclusive sample cuts are discussed 3.3.1. Since both flux and systematic weights are applied to all MC events in BANFF, it is important to validate the event weights. Using neither set of weights is referred to as the nominal MC.

ν_μ **FHC**: Shown inFigures 3.1 to 3.7 are the momentum and $\cos\theta$ distributions for ν_μCC-Inclusive events in FHC mode. There are three pairs of P, θ figures with the same truth information break down accompanied by one of neutrino energy. The truth information categories are lepton candidate particle, NEUT reaction, and topology. Each figure consists of a set of four sub-figures which illustrate the application of flux and detector systematic weights.
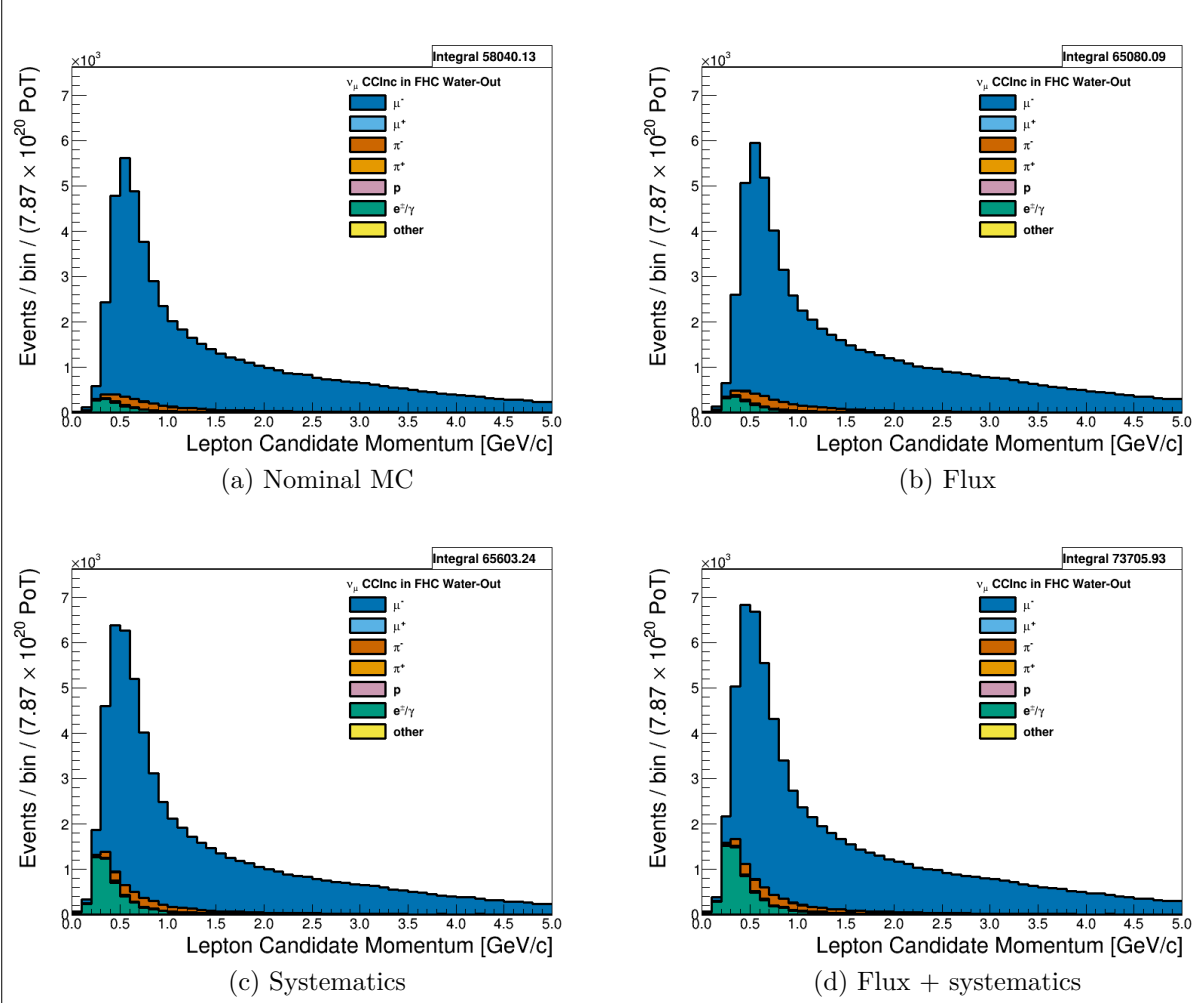
Figure 3.1: Reconstructed lepton candidate momentum separated by true particle species for FHC ν_μ CC-Inc. events occurring in the PØD in water-out mode. (a) The nominal MC prediction without any weights applied. (b) The flux tuning is applied. (c) The systematic weighting is applied. (d) Both flux and systematic weighting is applied.
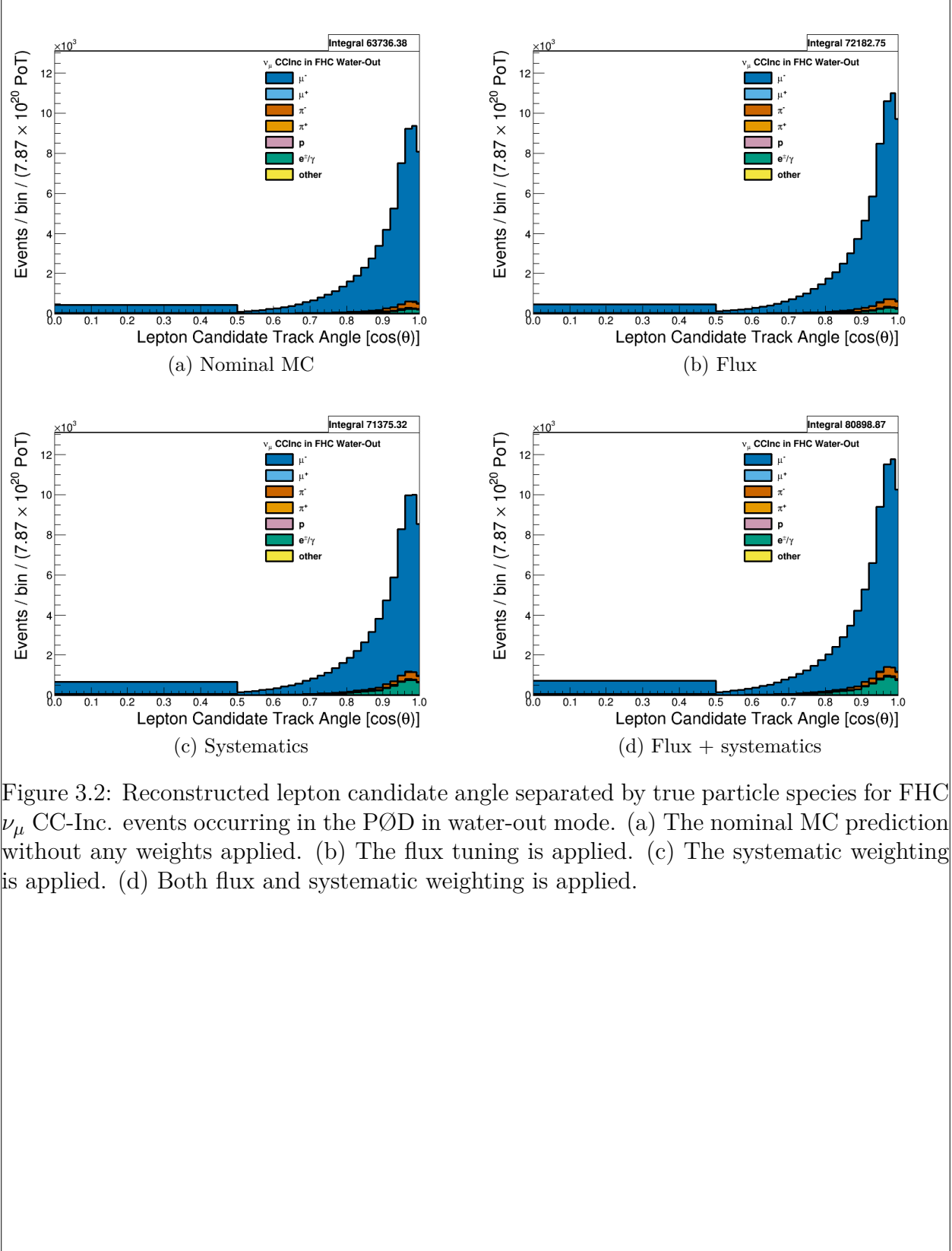
Figure 3.2: Reconstructed lepton candidate angle separated by true particle species for FHC ν_μ CC-Inc. events occurring in the PØD in water-out mode. (a) The nominal MC prediction without any weights applied. (b) The flux tuning is applied. (c) The systematic weighting is applied. (d) Both flux and systematic weighting is applied.
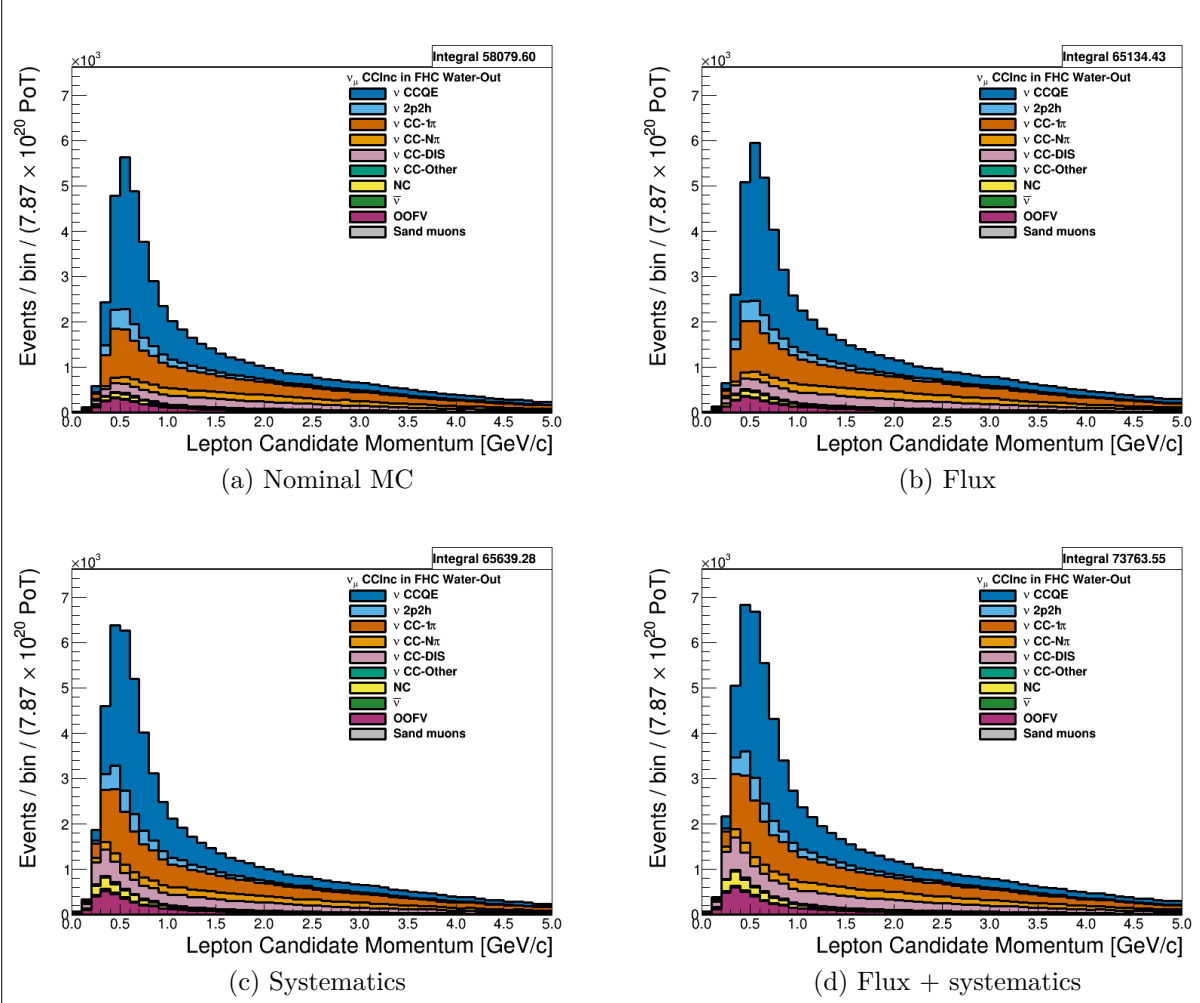
Figure 3.3: Reconstructed lepton candidate momentum separated by NEUT model interaction mode for FHC ν_μ CC-Inc. events occurring in the PØD in water-out mode. (a) The nominal MC prediction without any weights applied. (b) The flux tuning is applied. (c) The systematic weighting is applied. (d) Both flux and systematic weighting is applied.
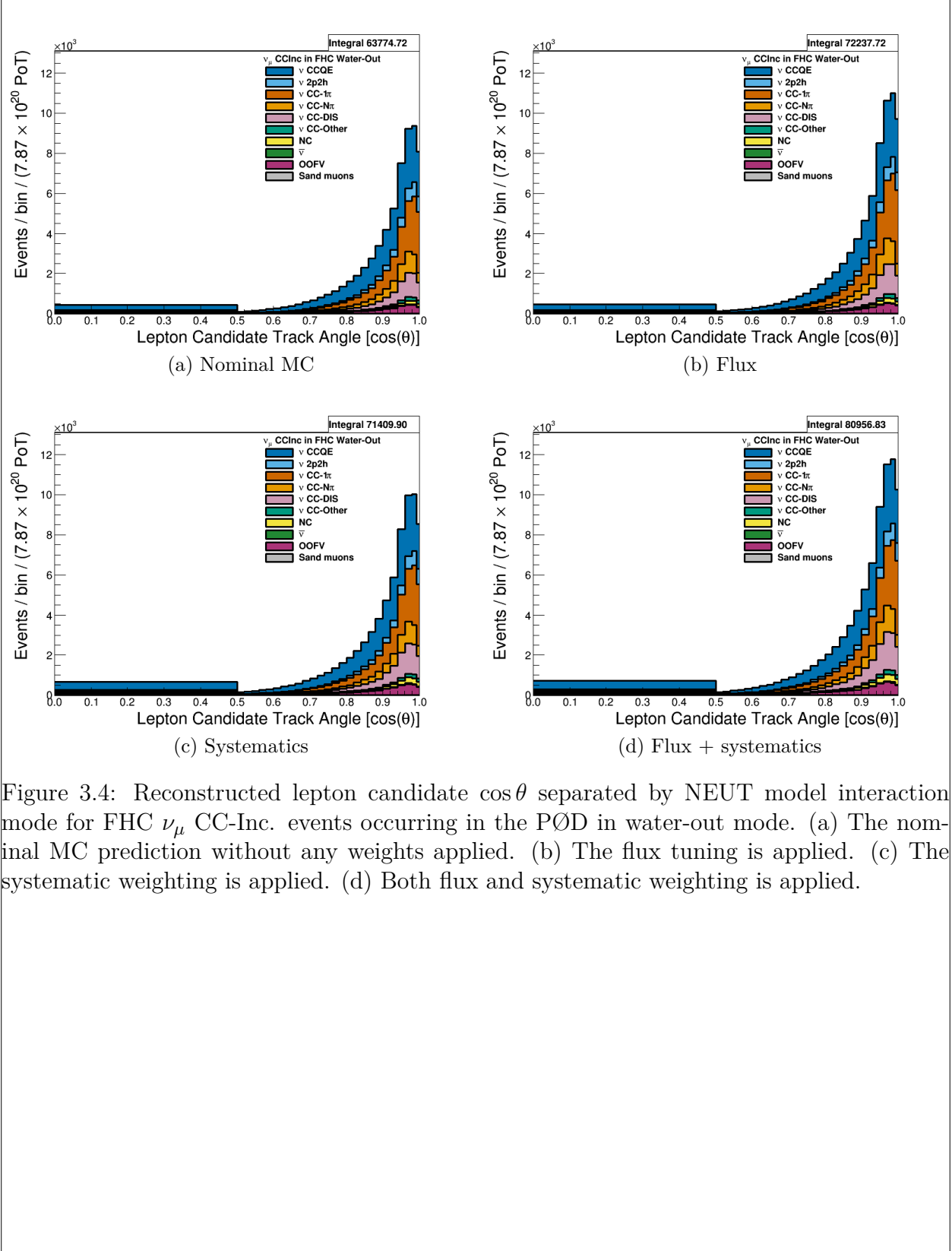
Figure 3.4: Reconstructed lepton candidate $\cos\theta$ separated by NEUT model interaction mode for FHC ν_μ CC-Inc. events occurring in the PØD in water-out mode. (a) The nominal MC prediction without any weights applied. (b) The flux tuning is applied. (c) The systematic weighting is applied. (d) Both flux and systematic weighting is applied.

(a) Nominal MC

(b) Flux

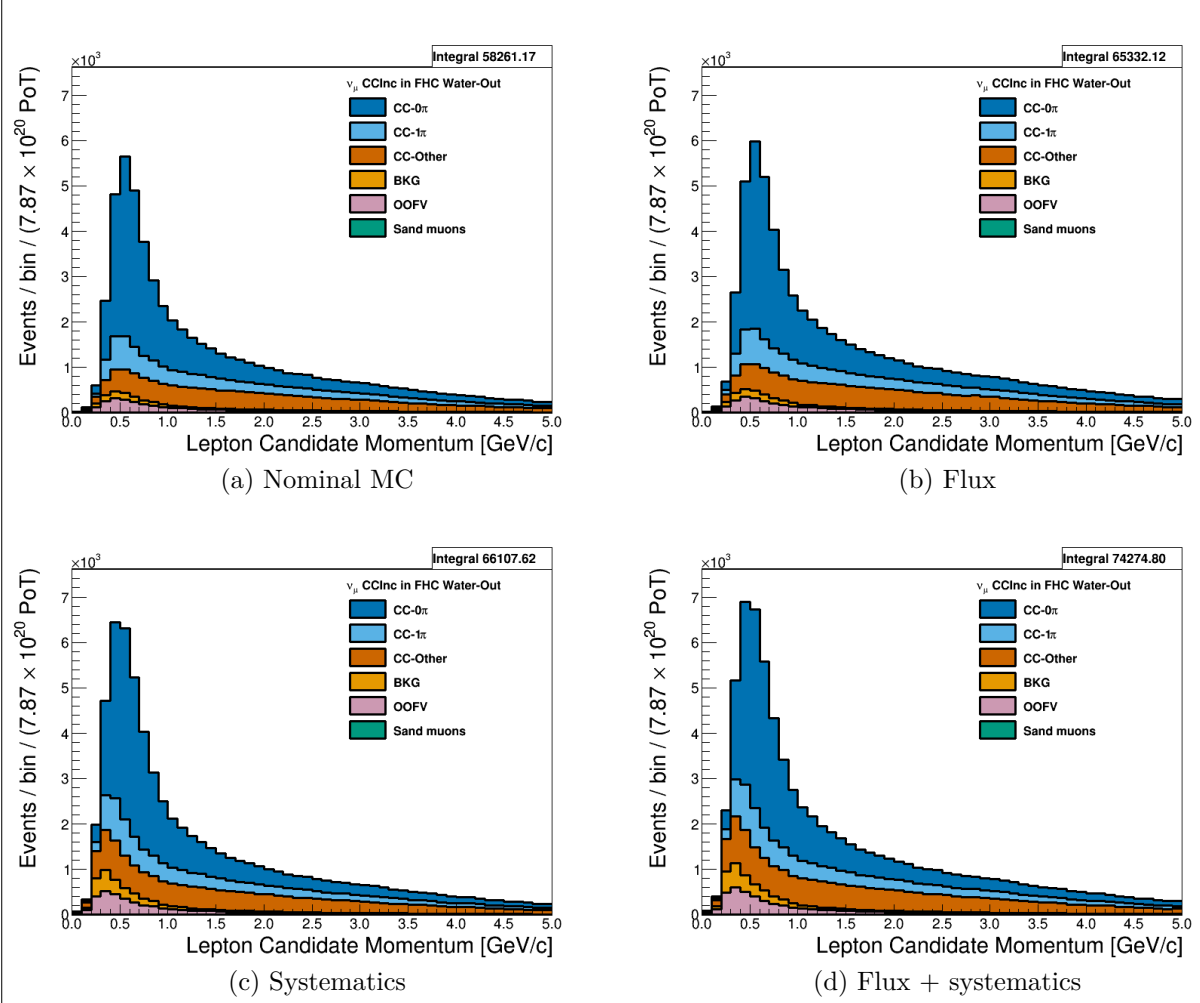(c) Systematics

(d) Flux + systematics

Figure 3.5: Reconstructed lepton candidate momentum separated by topology for FHC ν_μ CC-Inc. events occurring in the PØD in water-out mode. (a) The nominal MC prediction without any weights applied. (b) The flux tuning is applied. (c) The systematic weighting is applied. (d) Both flux and systematic weighting is applied.
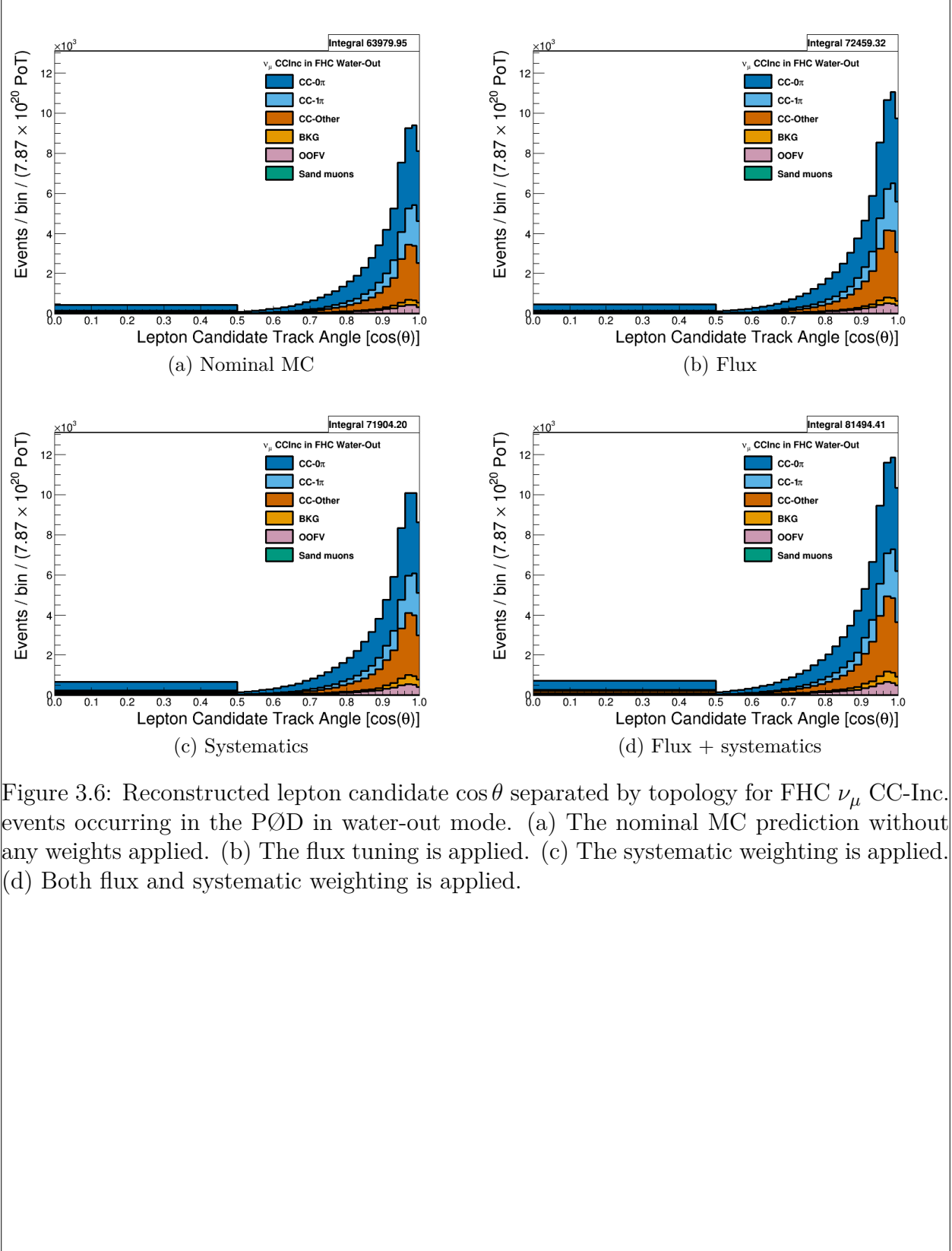
Figure 3.6: Reconstructed lepton candidate $\cos\theta$ separated by topology for FHC ν_μ CC-Inc. events occurring in the PØD in water-out mode. (a) The nominal MC prediction without any weights applied. (b) The flux tuning is applied. (c) The systematic weighting is applied. (d) Both flux and systematic weighting is applied.
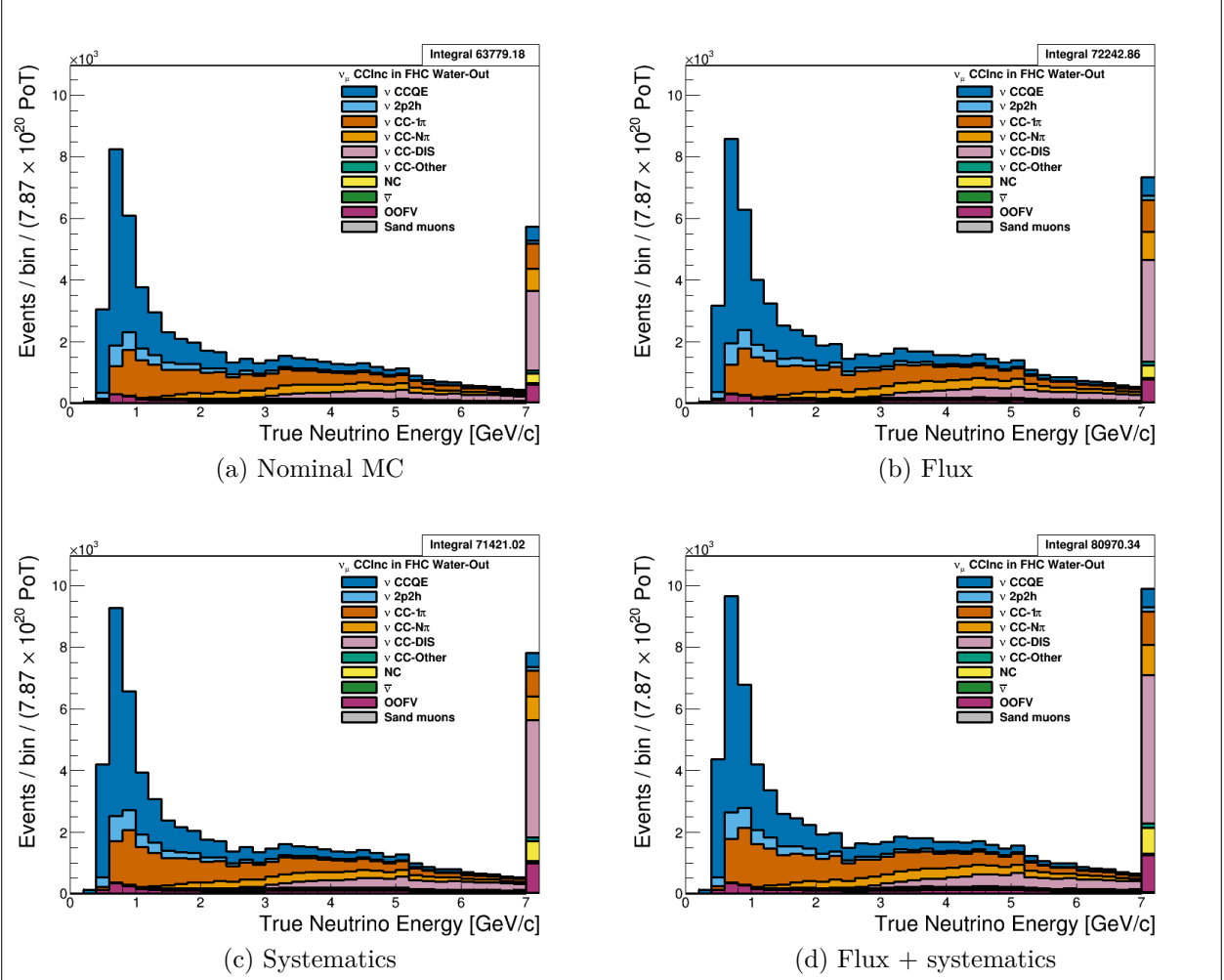
Figure 3.7: True neutrino energy associated with the lepton candidate separated by NEUT model interaction mode for FHC ν_μ CC-Inc. events occurring in the PØD in water-out mode. (a) The nominal MC prediction without any weights applied. (b) The flux tuning is applied. (c) The systematic weighting is applied. (d) Both flux and systematic weighting is applied.

$\overline{\nu}_\mu$ **RHC**: Shown in Figures 3.8 to 3.14 for $\overline{\nu}_\mu$CC-Inclusive events in RHC mode. There are three pairs of P, θ figures with the same truth information break down accompanied by one of neutrino energy. The truth information categories are lepton candidate particle, NEUT reaction, and topology. Each figure consists of a set of four sub-figures which illustrate the application of flux and detector systematic weights.
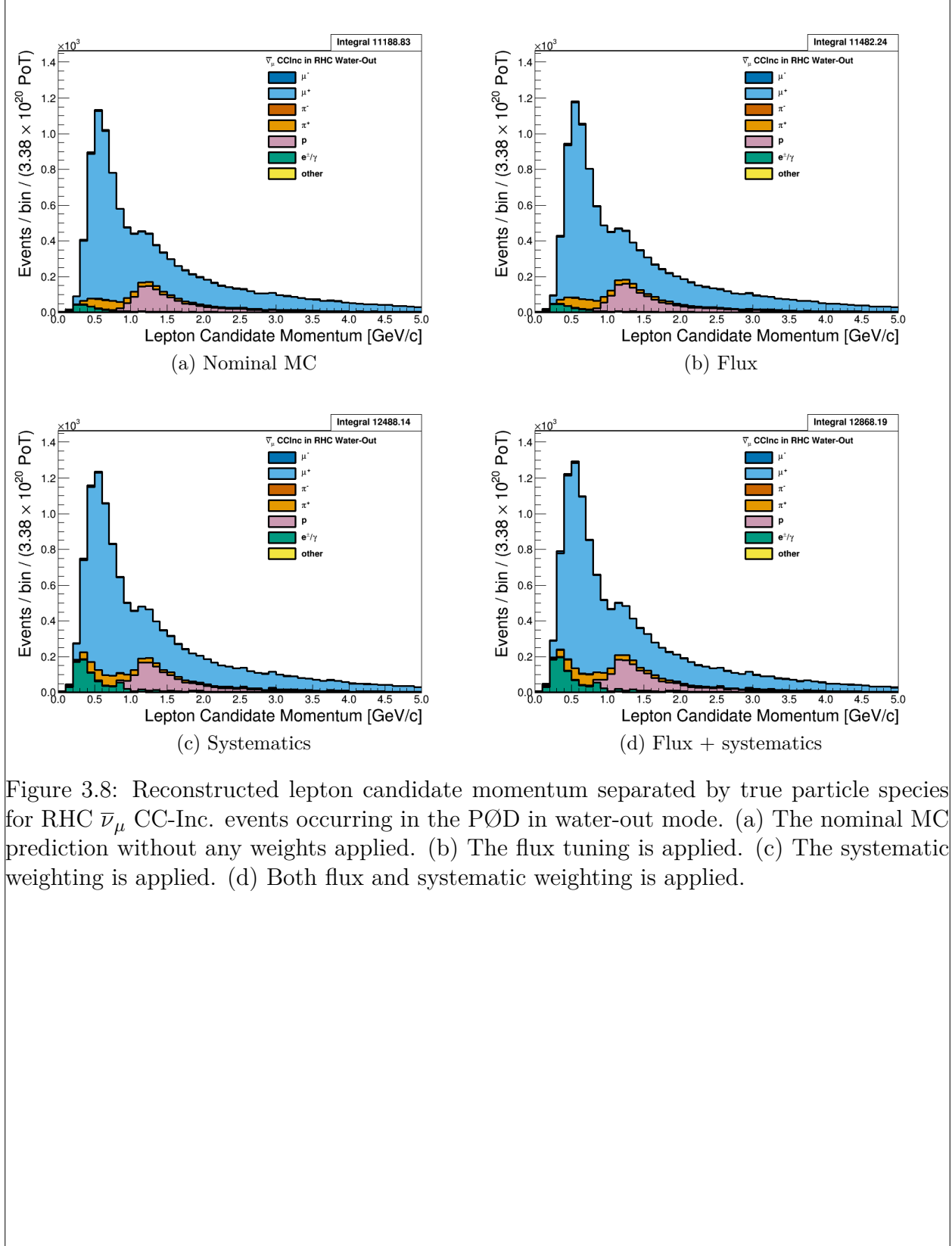
Figure 3.8: Reconstructed lepton candidate momentum separated by true particle species for RHC $\overline{\nu}_\mu$ CC-Inc. events occurring in the PØD in water-out mode. (a) The nominal MC prediction without any weights applied. (b) The flux tuning is applied. (c) The systematic weighting is applied. (d) Both flux and systematic weighting is applied.

(a) Nominal MC

(b) Flux

(c) Systematics

(d) Flux + systematics

Figure 3.9: Reconstructed lepton candidate angle separated by true particle species for RHC $\overline{\nu}_\mu$ CC-Inc. events occurring in the PØD in water-out mode. (a) The nominal MC prediction without any weights applied. (b) The flux tuning is applied. (c) The systematic weighting is applied. (d) Both flux and systematic weighting is applied.
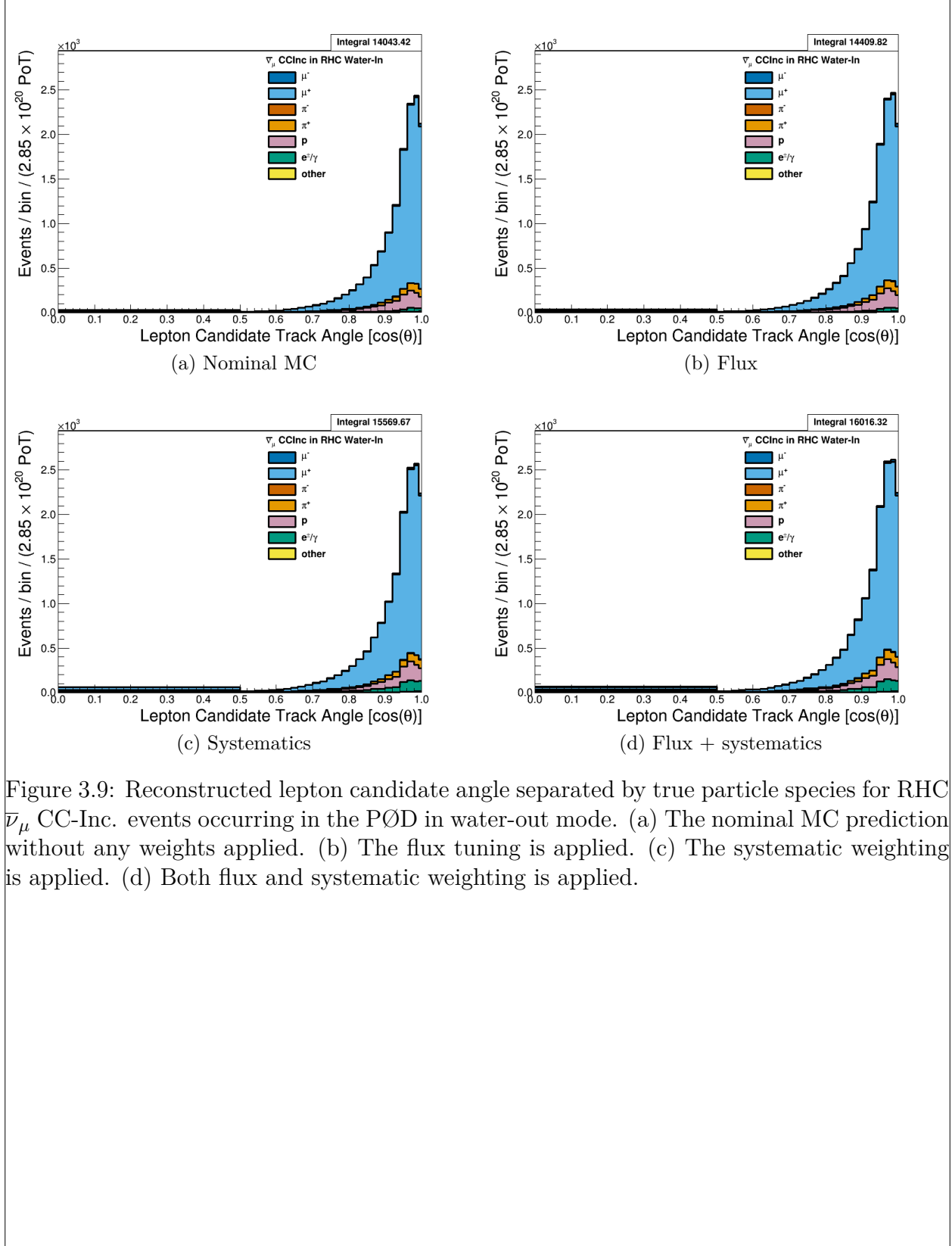
Figure 3.10: Reconstructed lepton candidate momentum separated by NEUT model interaction mode for RHC $\overline{\nu}_\mu$ CC-Inc. events occurring in the PØD in water-out mode. (a) The nominal MC prediction without any weights applied. (b) The flux tuning is applied. (c) The systematic weighting is applied. (d) Both flux and systematic weighting is applied.
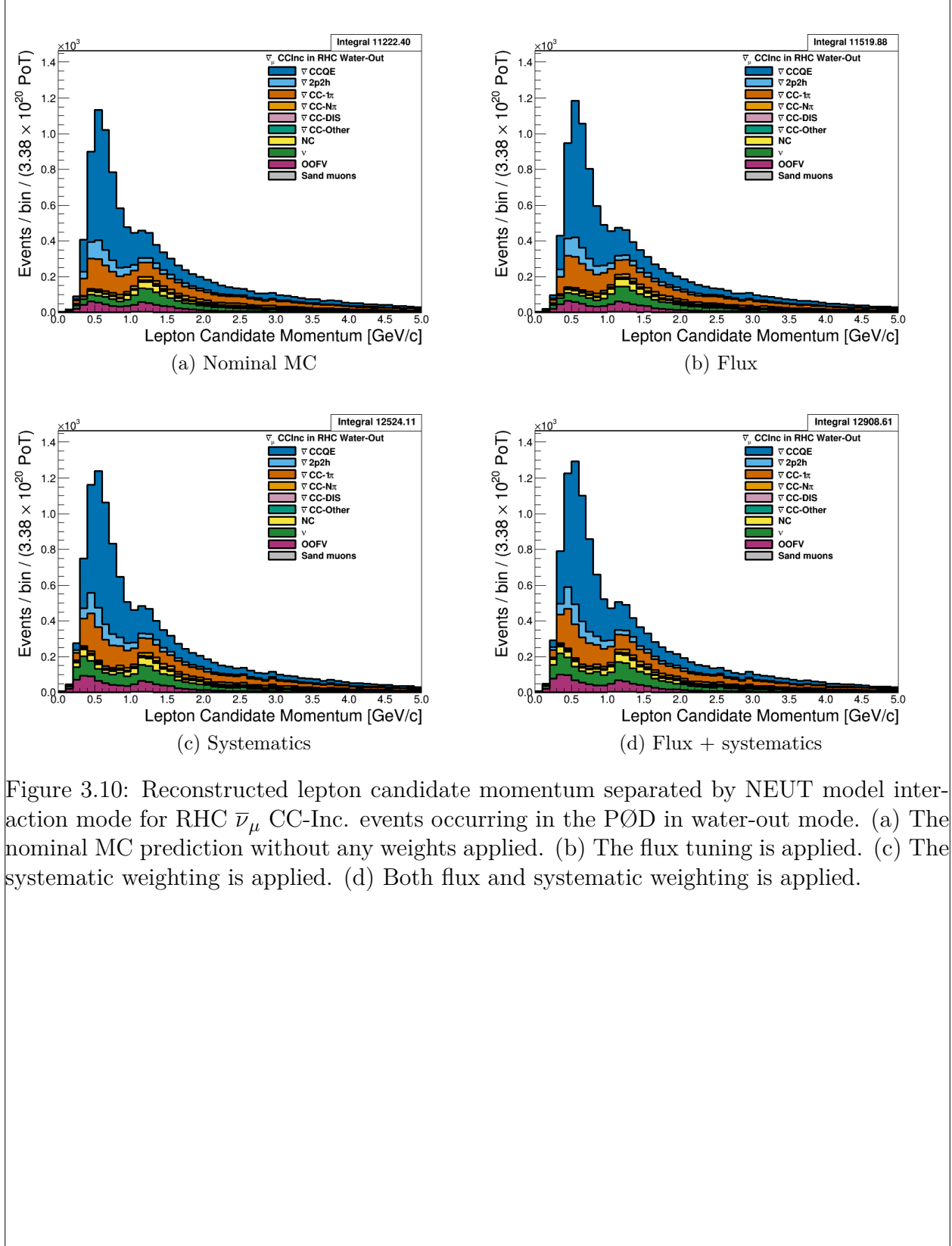
Figure 3.11: Reconstructed lepton candidate $\cos\theta$ separated by NEUT model interaction mode for RHC $\overline{\nu}_\mu$ CC-Inc. events occurring in the PØD in water-out mode. (a) The nominal MC prediction without any weights applied. (b) The flux tuning is applied. (c) The systematic weighting is applied. (d) Both flux and systematic weighting is applied.
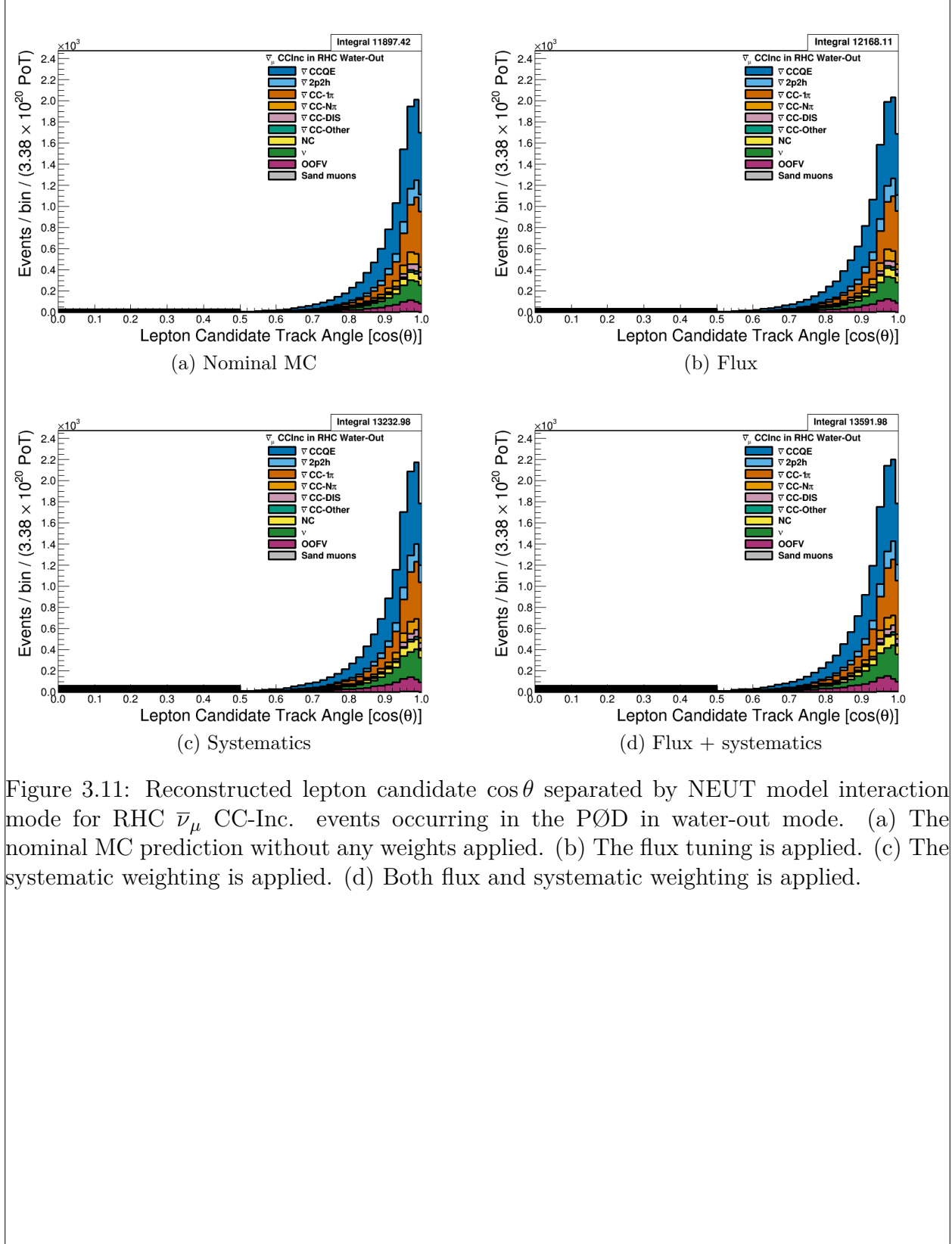
(a) Nominal MC

(b) Flux

(c) Systematics

(d) Flux + systematics

Figure 3.12: Reconstructed lepton candidate momentum separated by topology for RHC $\overline{\nu}_\mu$ CC-Inc. events occurring in the PØD in water-out mode. (a) The nominal MC prediction without any weights applied. (b) The flux tuning is applied. (c) The systematic weighting is applied. (d) Both flux and systematic weighting is applied.
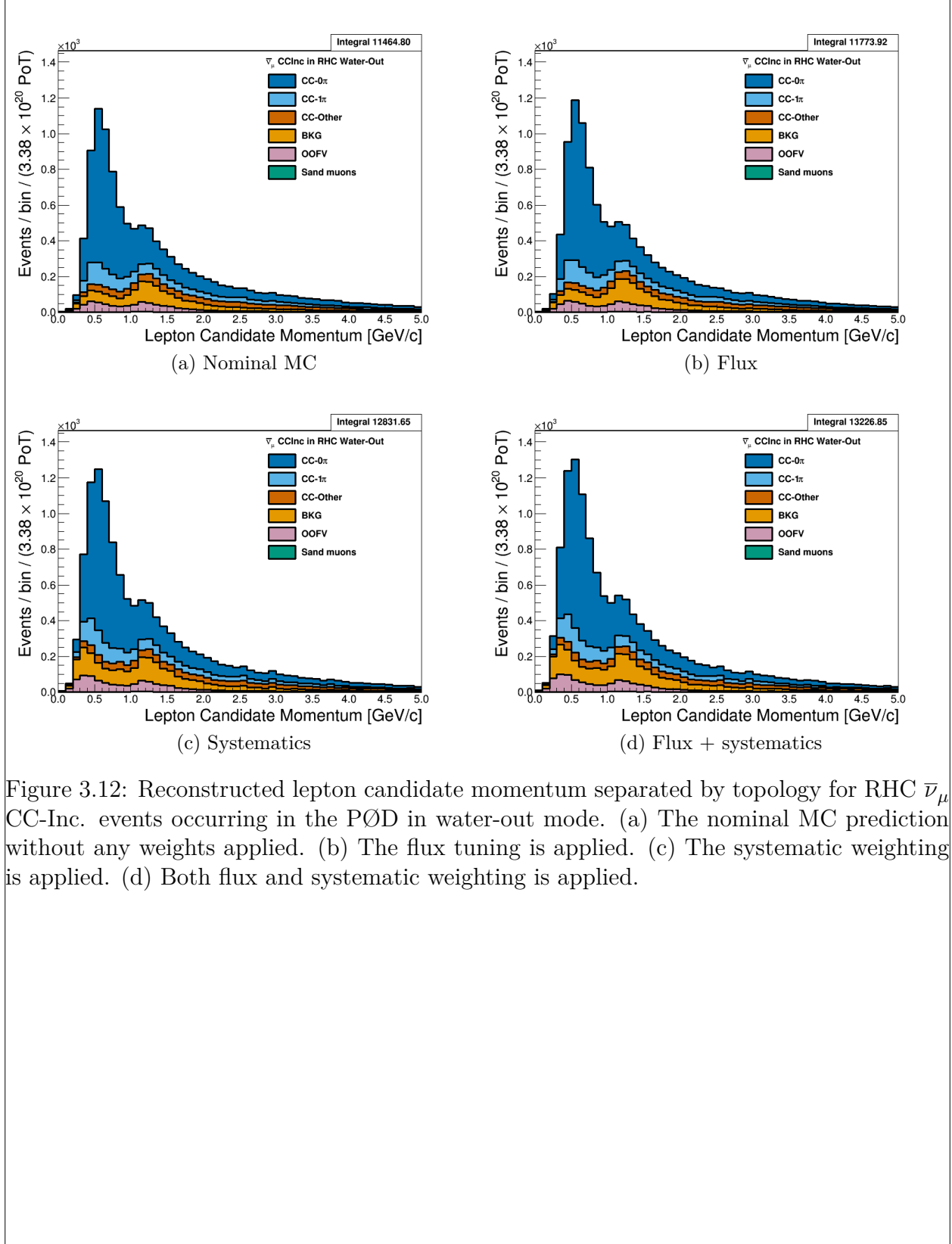
Figure 3.13: Reconstructed lepton candidate $\cos\theta$ separated by topology for RHC $\overline{\nu}_\mu$ CC-Inc. events occurring in the PØD in water-out mode. (a) The nominal MC prediction without any weights applied. (b) The flux tuning is applied. (c) The systematic weighting is applied. (d) Both flux and systematic weighting is applied.
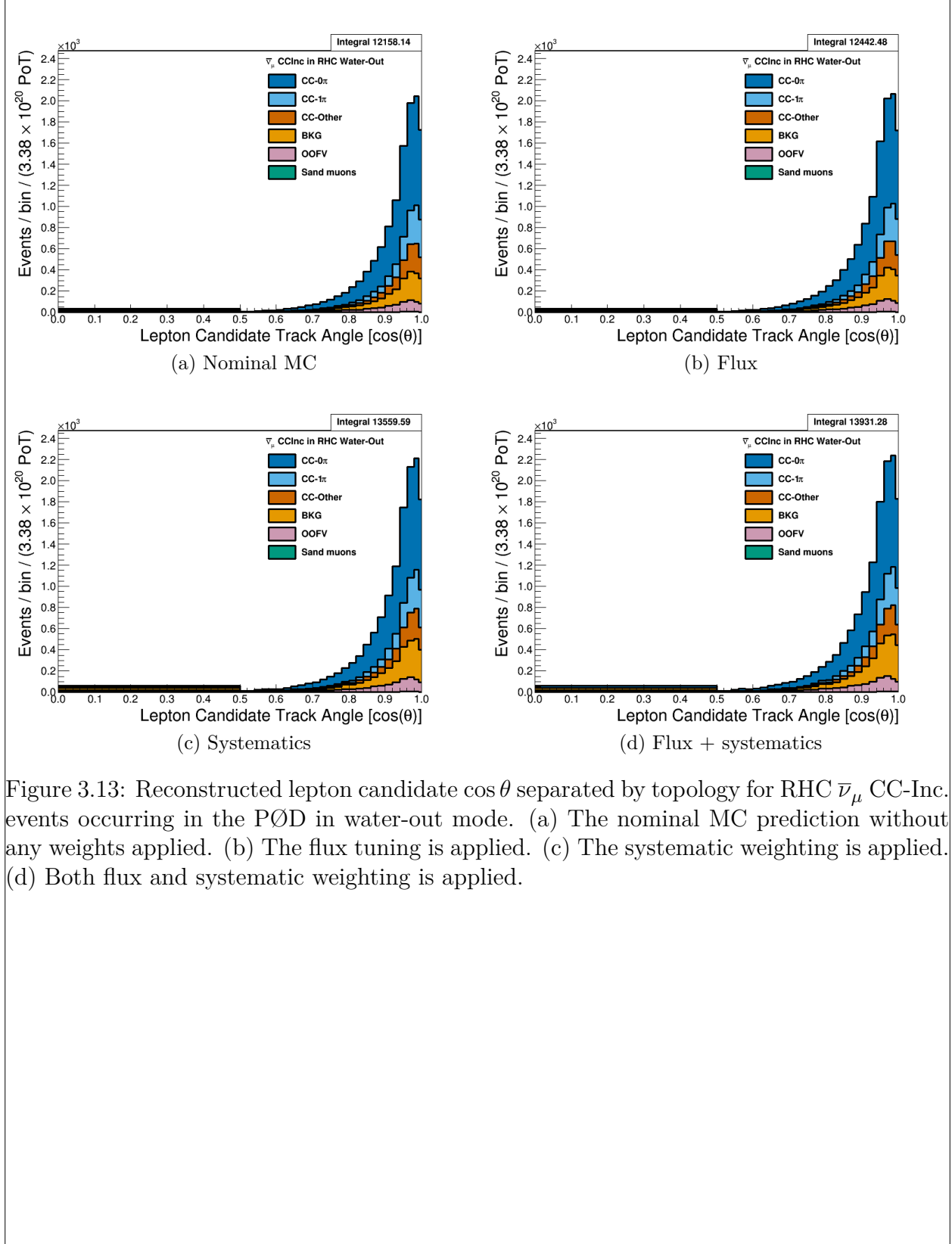
Figure 3.14: True neutrino energy associated with the lepton candidate separated by NEUT model interaction mode for RHC $\overline{\nu}_\mu$ CC-Inc. events occurring in the PØD in water-out mode. (a) The nominal MC prediction without any weights applied. (b) The flux tuning is applied. (c) The systematic weighting is applied. (d) Both flux and systematic weighting is applied.
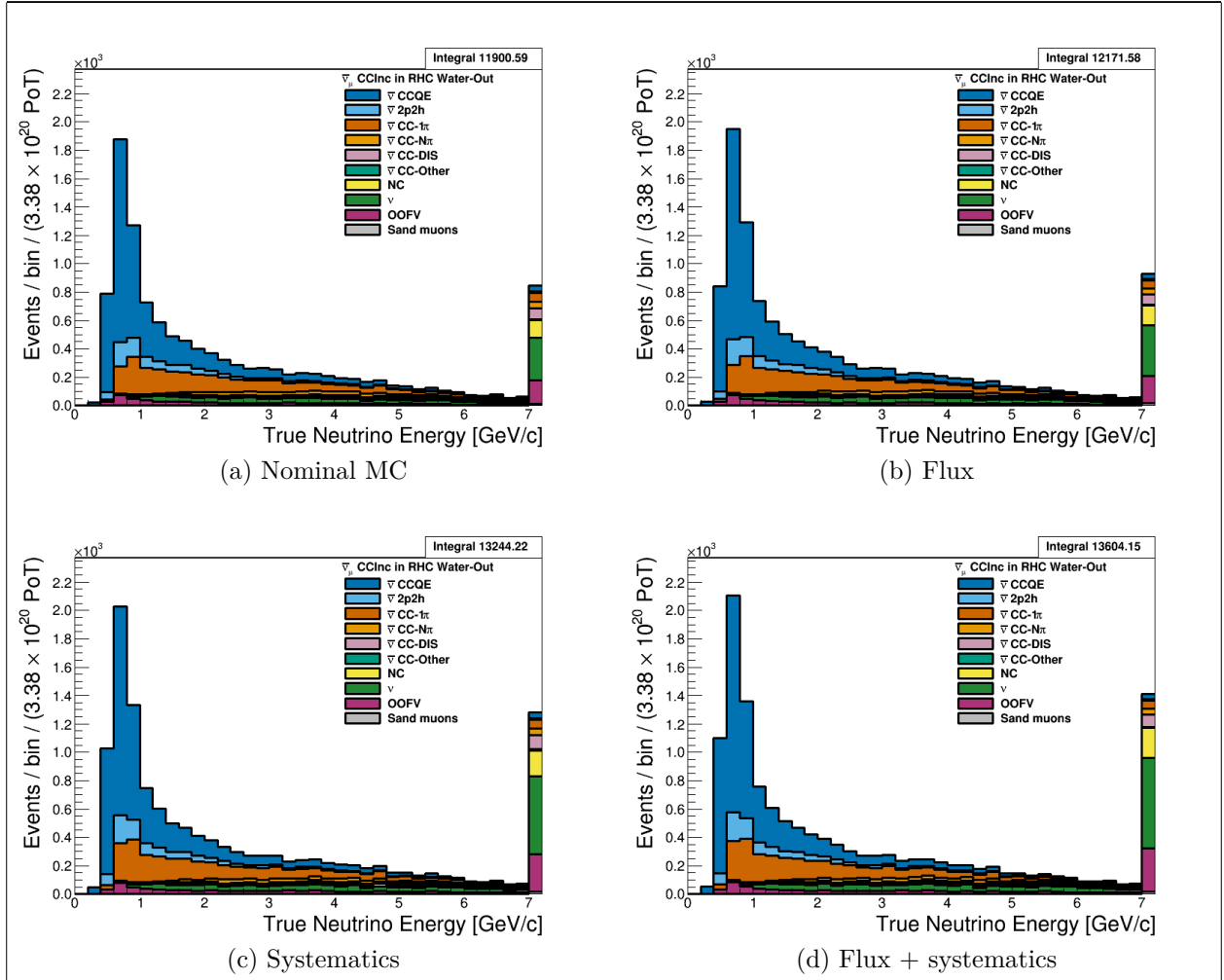
$\boldsymbol{\nu_\mu}$ **RHC**:Add figures here

3.4.2   CC-1 Track (CCQE Enhanced)

Add figures here

3.4.3   CC-N Tracks (CCnQE Enhanced)

3.5 PØD Water-In Samples

This section shows the kinematic distributions for the PØD water-in samples. These samples will demonstrate the similarities between it and water-out modes. First an examination of the CC-Inclusive samples and the effects of the systematic weights will be explored. The samples are then examined as CC 1-track and CC N-tracks.

3.5.1 CC-Inclusive

The CC-Inclusive sample cuts are discussed 3.3.1. Since both flux and detector systematic weights are applied to all MC events in BANFF, it is important to validate the event weights. Using neither set of weights is referred to as the nominal MC.

ν_μ **FHC**: Shown in Figures 3.15 to 3.21 are the momentum and $\cos\theta$ distributions for ν_μCC-Inclusive events in FHC mode. There are three pairs of P, θ figures with the same truth information break down accompanied by one of neutrino energy. The truth information categories are lepton candidate particle, NEUT reaction, and topology. Each figure consists of a set of four sub-figures which illustrate the application of flux and detector systematic weights.
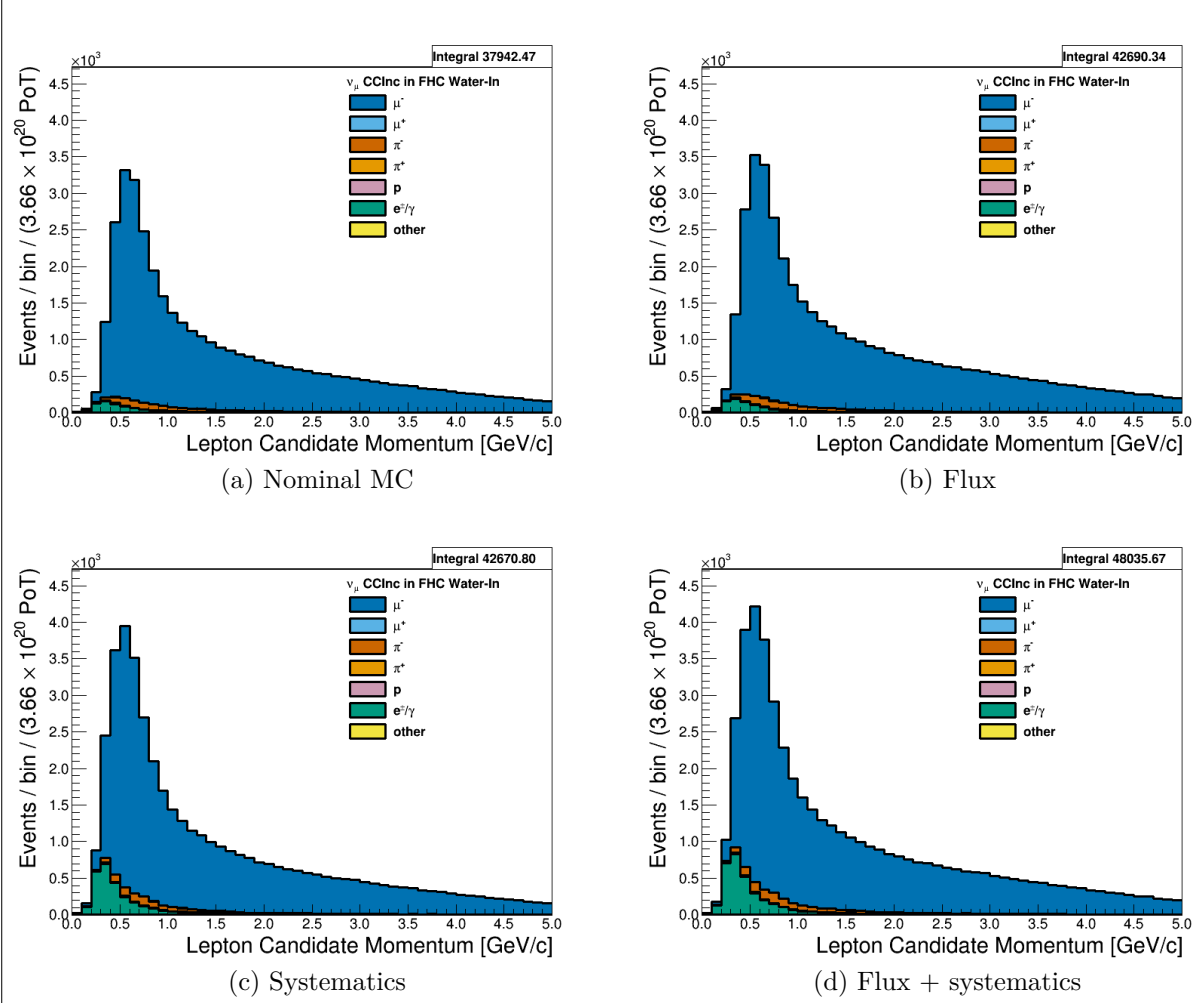
Figure 3.15: Reconstructed lepton candidate momentum separated by true particle species for FHC ν_μ CC-Inc. events occurring in the PØD in water-in mode. (a) The nominal MC prediction without any weights applied. (b) The flux tuning is applied. (c) The systematic weighting is applied. (d) Both flux and systematic weighting is applied.

(a) Nominal MC

(b) Flux
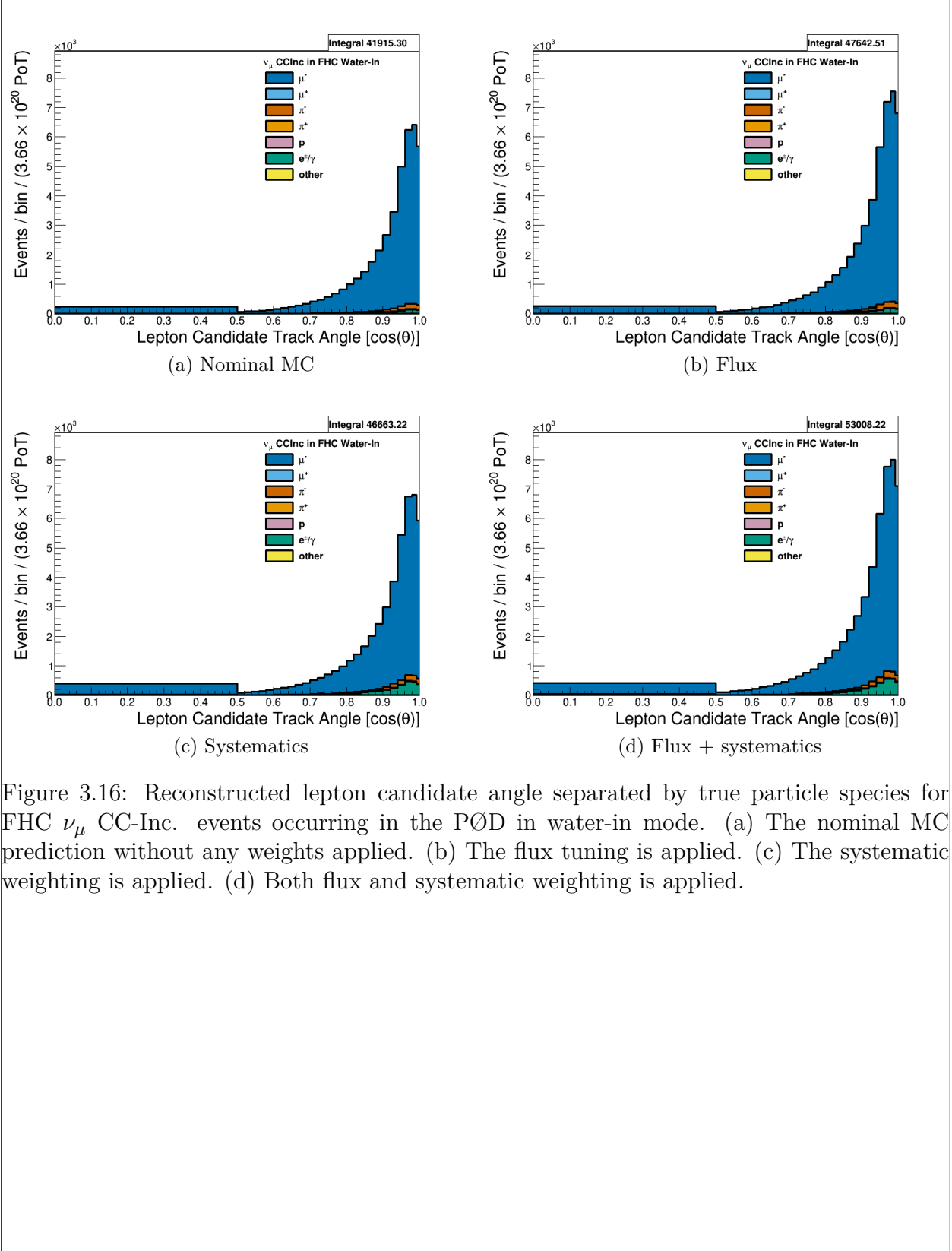
(c) Systematics

(d) Flux + systematics

Figure 3.16: Reconstructed lepton candidate angle separated by true particle species for FHC ν_μ CC-Inc. events occurring in the PØD in water-in mode. (a) The nominal MC prediction without any weights applied. (b) The flux tuning is applied. (c) The systematic weighting is applied. (d) Both flux and systematic weighting is applied.

(a) Nominal MC

(b) Flux
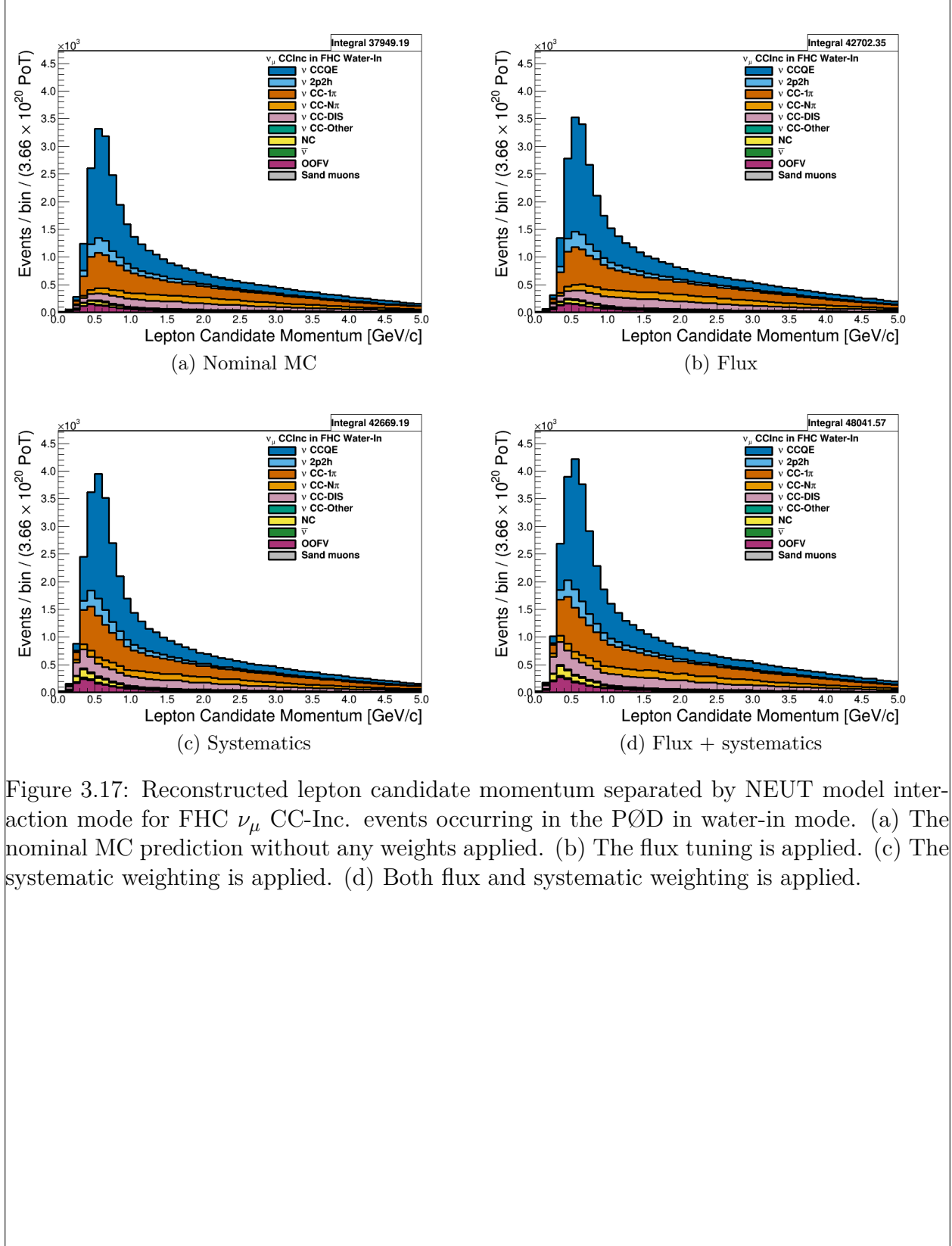
(c) Systematics

(d) Flux + systematics

Figure 3.17: Reconstructed lepton candidate momentum separated by NEUT model interaction mode for FHC ν_μ CC-Inc. events occurring in the PØD in water-in mode. (a) The nominal MC prediction without any weights applied. (b) The flux tuning is applied. (c) The systematic weighting is applied. (d) Both flux and systematic weighting is applied.

(a) Nominal MC

(b) Flux
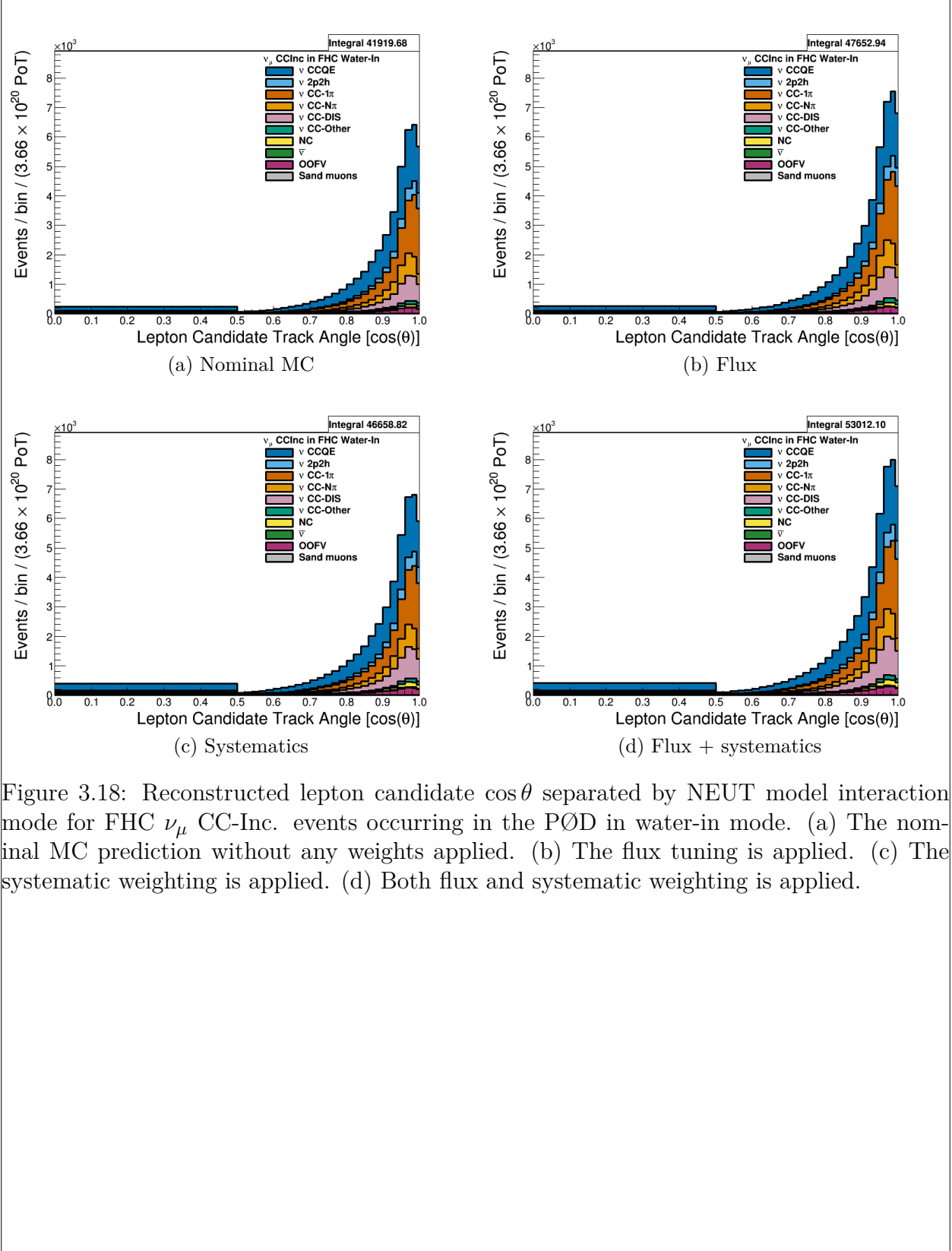
(c) Systematics

(d) Flux + systematics

Figure 3.18: Reconstructed lepton candidate $\cos\theta$ separated by NEUT model interaction mode for FHC ν_μ CC-Inc. events occurring in the PØD in water-in mode. (a) The nominal MC prediction without any weights applied. (b) The flux tuning is applied. (c) The systematic weighting is applied. (d) Both flux and systematic weighting is applied.
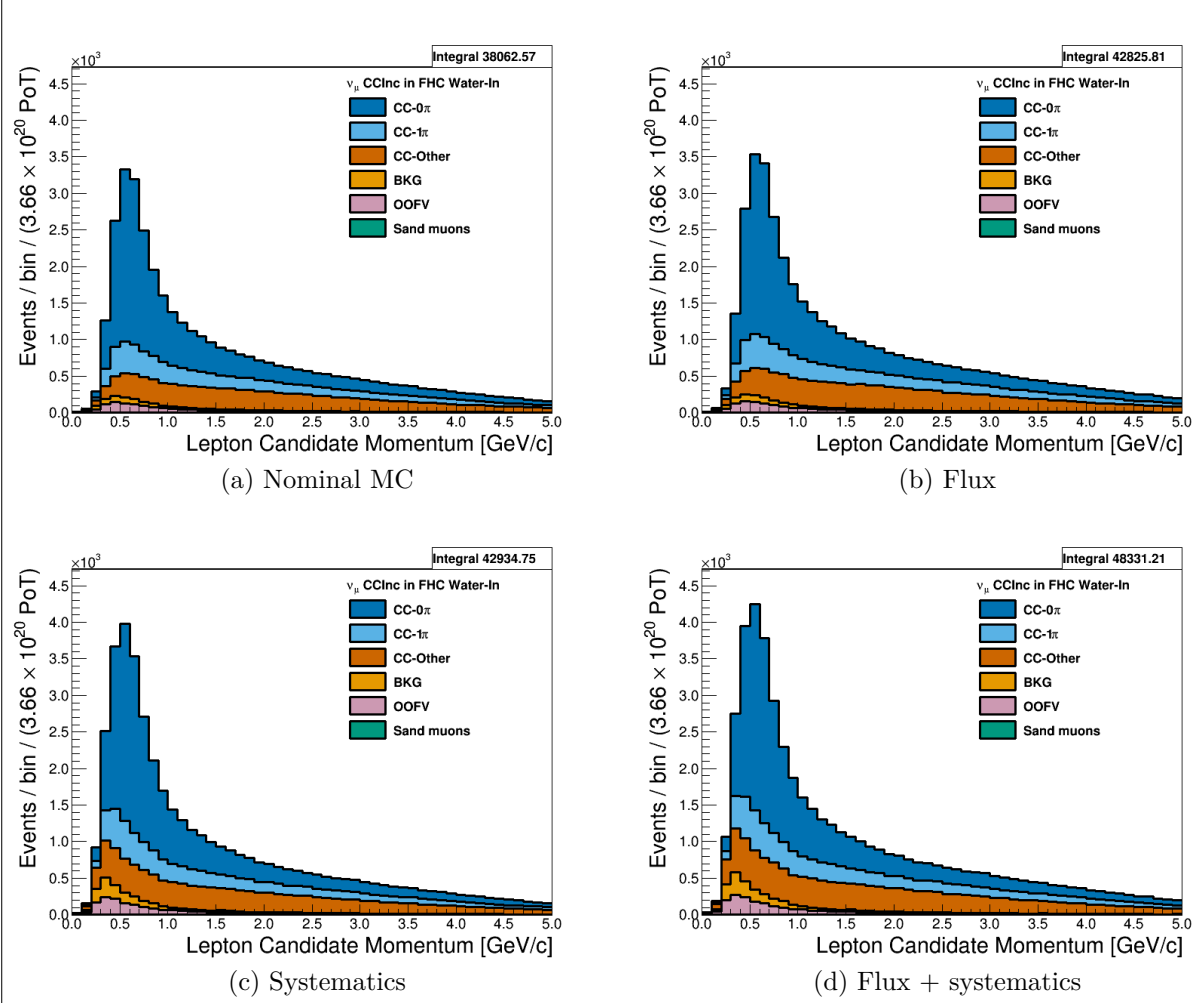
Figure 3.19: Reconstructed lepton candidate momentum separated by topology for FHC ν_μ CC-Inc. events occurring in the PØD in water-in mode. (a) The nominal MC prediction without any weights applied. (b) The flux tuning is applied. (c) The systematic weighting is applied. (d) Both flux and systematic weighting is applied.
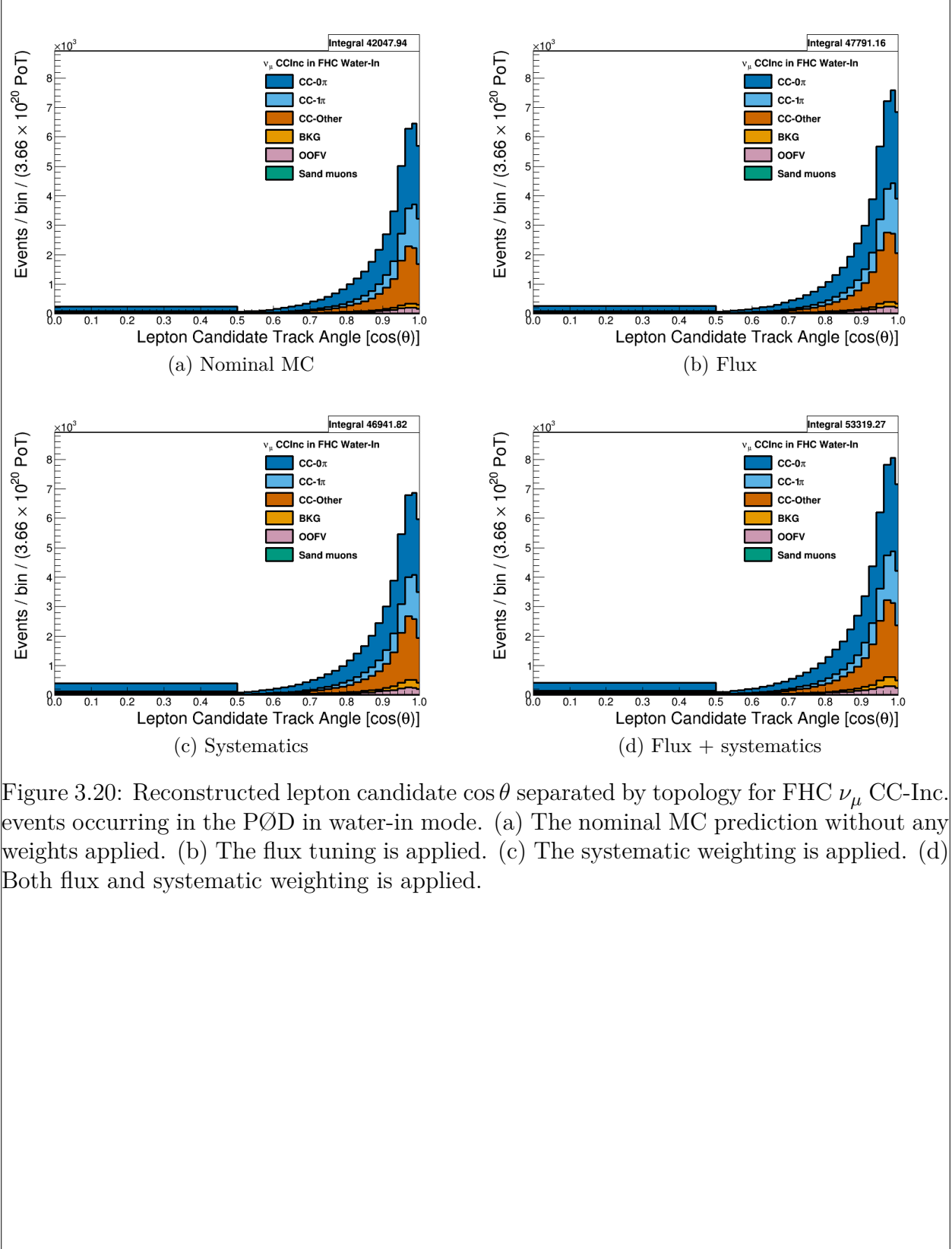
Figure 3.20: Reconstructed lepton candidate $\cos\theta$ separated by topology for FHC ν_μ CC-Inc. events occurring in the PØD in water-in mode. (a) The nominal MC prediction without any weights applied. (b) The flux tuning is applied. (c) The systematic weighting is applied. (d) Both flux and systematic weighting is applied.

(a) Nominal MC

(b) Flux
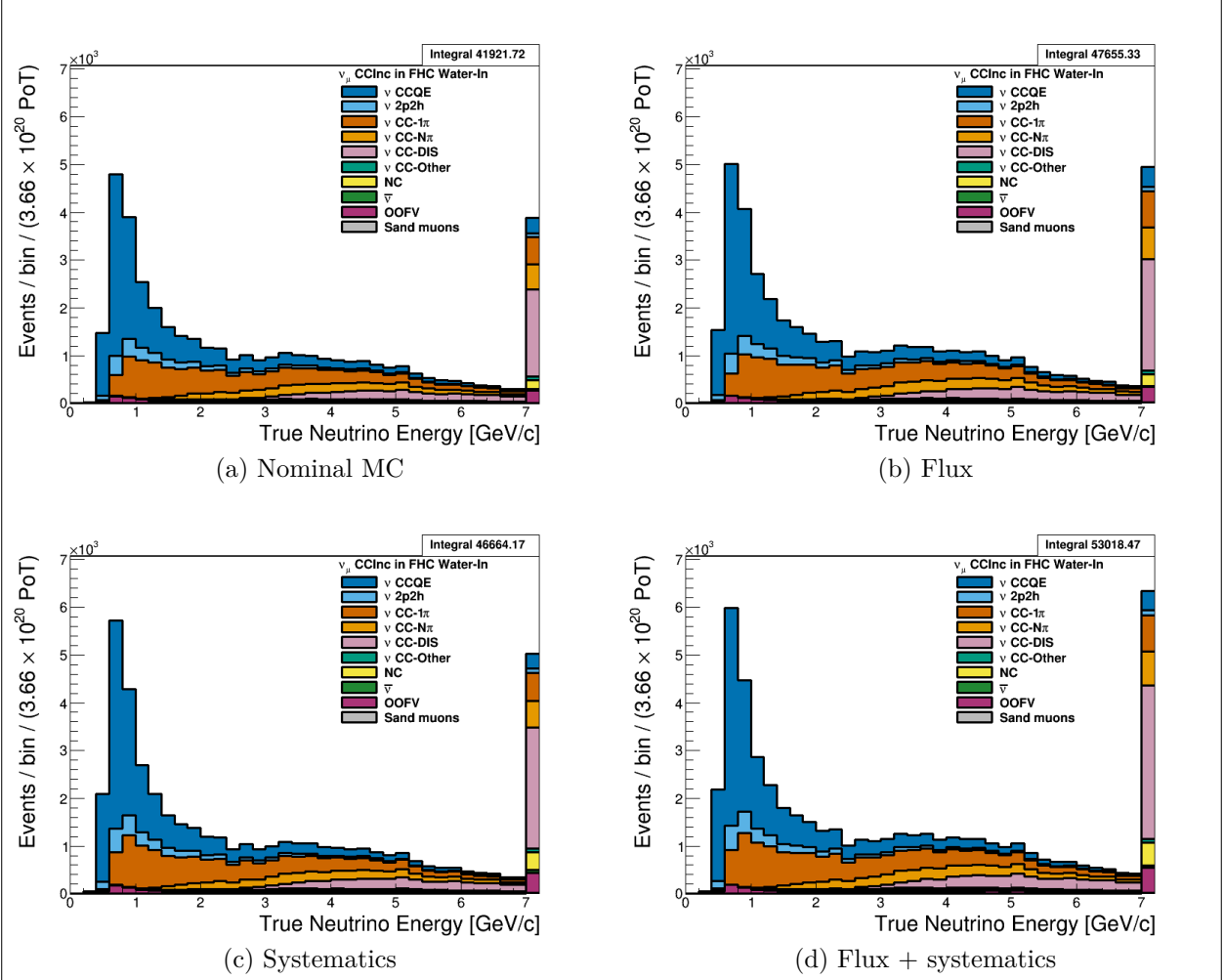
(c) Systematics

(d) Flux + systematics

Figure 3.21: True neutrino energy associated with the lepton candidate separated by NEUT model interaction mode for FHC ν_μ CC-Inc. events occurring in the PØD in water-out mode. (a) The nominal MC prediction without any weights applied. (b) The flux tuning is applied. (c) The systematic weighting is applied. (d) Both flux and systematic weighting is applied.

$\overline{\nu}_\mu$ **RHC**: Shown in Figures 3.22 to 3.28 for $\overline{\nu}_\mu$CC-Inclusive events in RHC mode. There are three pairs of P, θ figures with the same truth information break down accompanied by one of neutrino energy. The truth information categories are lepton candidate particle, NEUT reaction, and topology. Each figure consists of a set of four sub-figures which illustrate the application of flux and detector systematic weights.

(a) Nominal MC

(b) Flux

(c) Systematics

(d) Flux + systematics

Figure 3.22: Reconstructed lepton candidate momentum separated by true particle species for RHC $\overline{\nu}_\mu$ CC-Inc. events occurring in the PØD in water-out mode. (a) The nominal MC prediction without any weights applied. (b) The flux tuning is applied. (c) The systematic weighting is applied. (d) Both flux and systematic weighting is applied.

(a) Nominal MC

(b) Flux
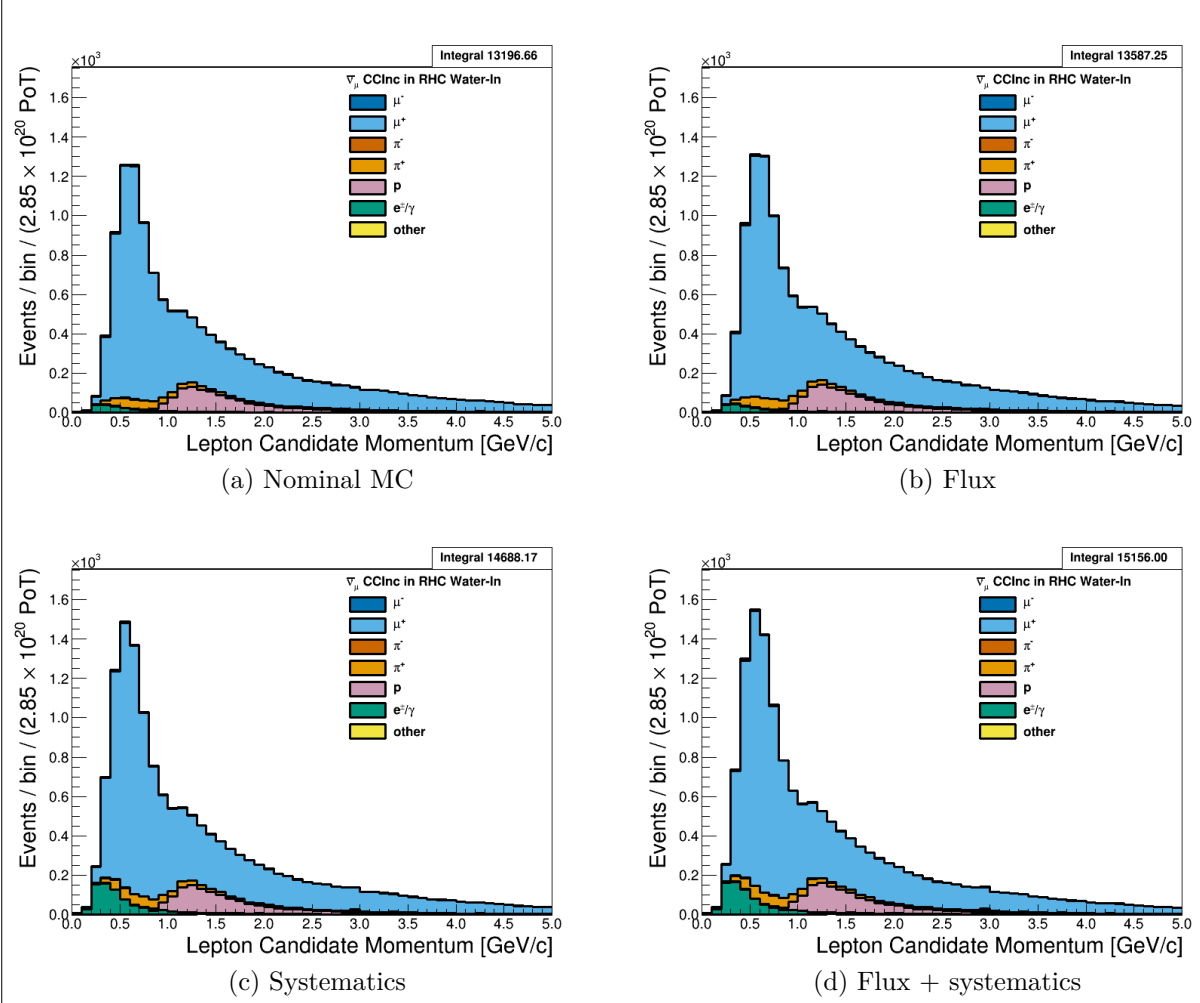
(c) Systematics

(d) Flux + systematics

Figure 3.23: Reconstructed lepton candidate angle separated by true particle species for RHC $\overline{\nu}_\mu$ CC-Inc. events occurring in the PØD in water-out mode. (a) The nominal MC prediction without any weights applied. (b) The flux tuning is applied. (c) The systematic weighting is applied. (d) Both flux and systematic weighting is applied.

(a) Nominal MC

(b) Flux

(c) Systematics

(d) Flux + systematics

Figure 3.24: Reconstructed lepton candidate momentum separated by NEUT model inter-action mode for RHC $\overline{\nu}_\mu$ CC-Inc. events occurring in the PØD in water-out mode. (a) The nominal MC prediction without any weights applied. (b) The flux tuning is applied. (c) The systematic weighting is applied. (d) Both flux and systematic weighting is applied.
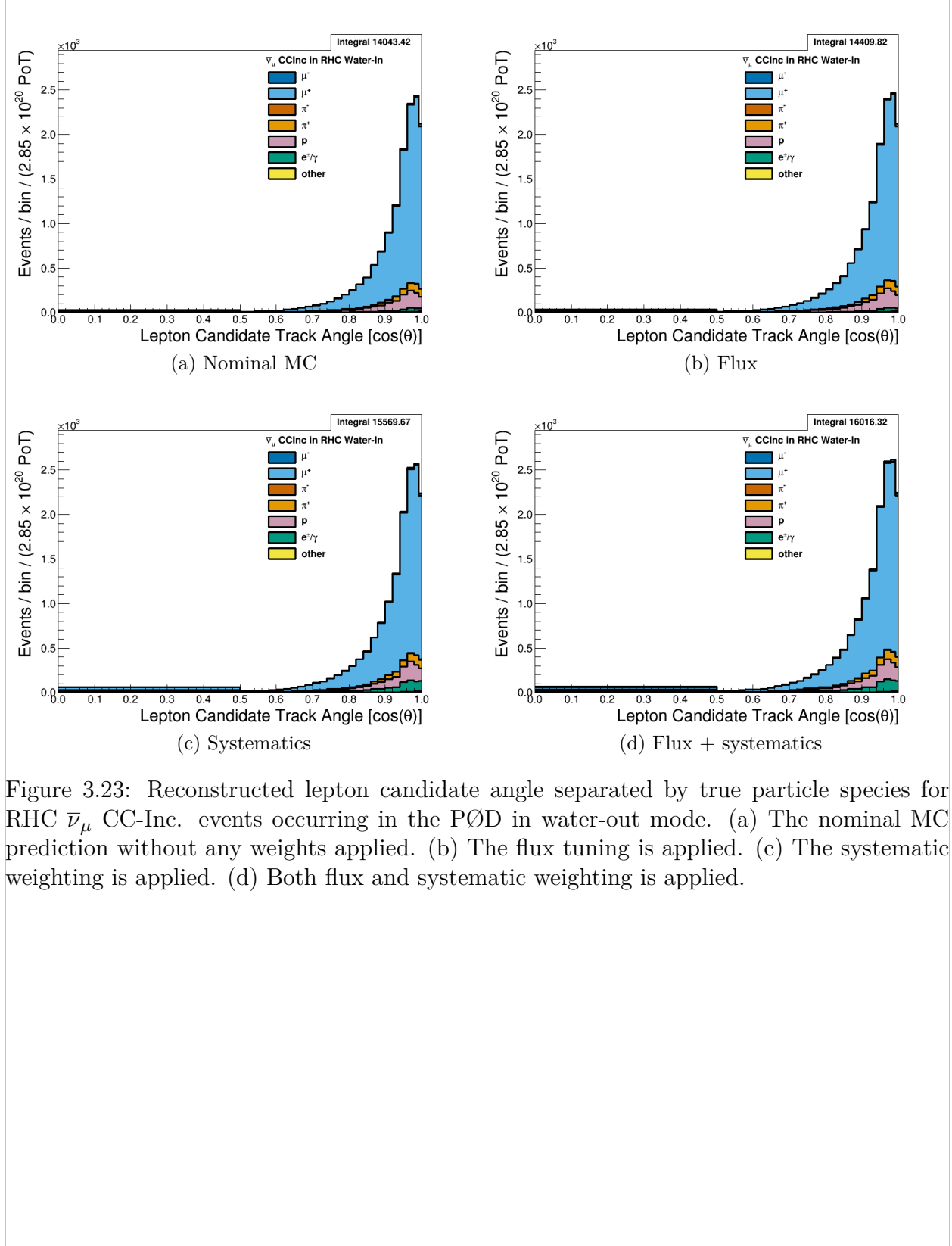
Figure 3.25: Reconstructed lepton candidate $\cos\theta$ separated by NEUT model interaction mode for RHC $\overline{\nu}_\mu$ CC-Inc. events occurring in the PØD in water-out mode. (a) The nominal MC prediction without any weights applied. (b) The flux tuning is applied. (c) The systematic weighting is applied. (d) Both flux and systematic weighting is applied.
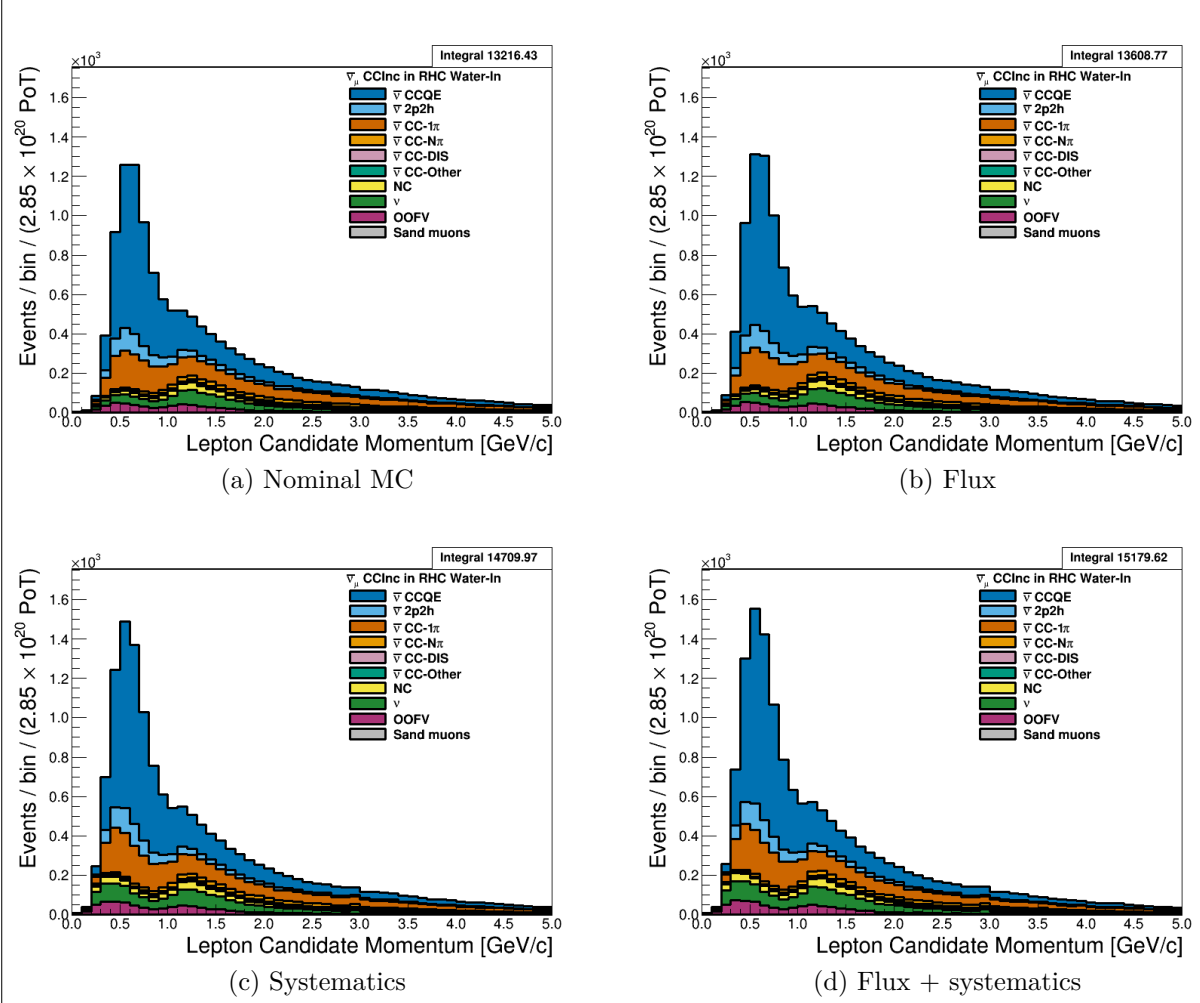
(a) Nominal MC

(b) Flux

(c) Systematics

(d) Flux + systematics

Figure 3.26: Reconstructed lepton candidate momentum separated by topology for RHC $\overline{\nu}_\mu$ CC-Inc. events occurring in the PØD in water-out mode. (a) The nominal MC prediction without any weights applied. (b) The flux tuning is applied. (c) The systematic weighting is applied. (d) Both flux and systematic weighting is applied.
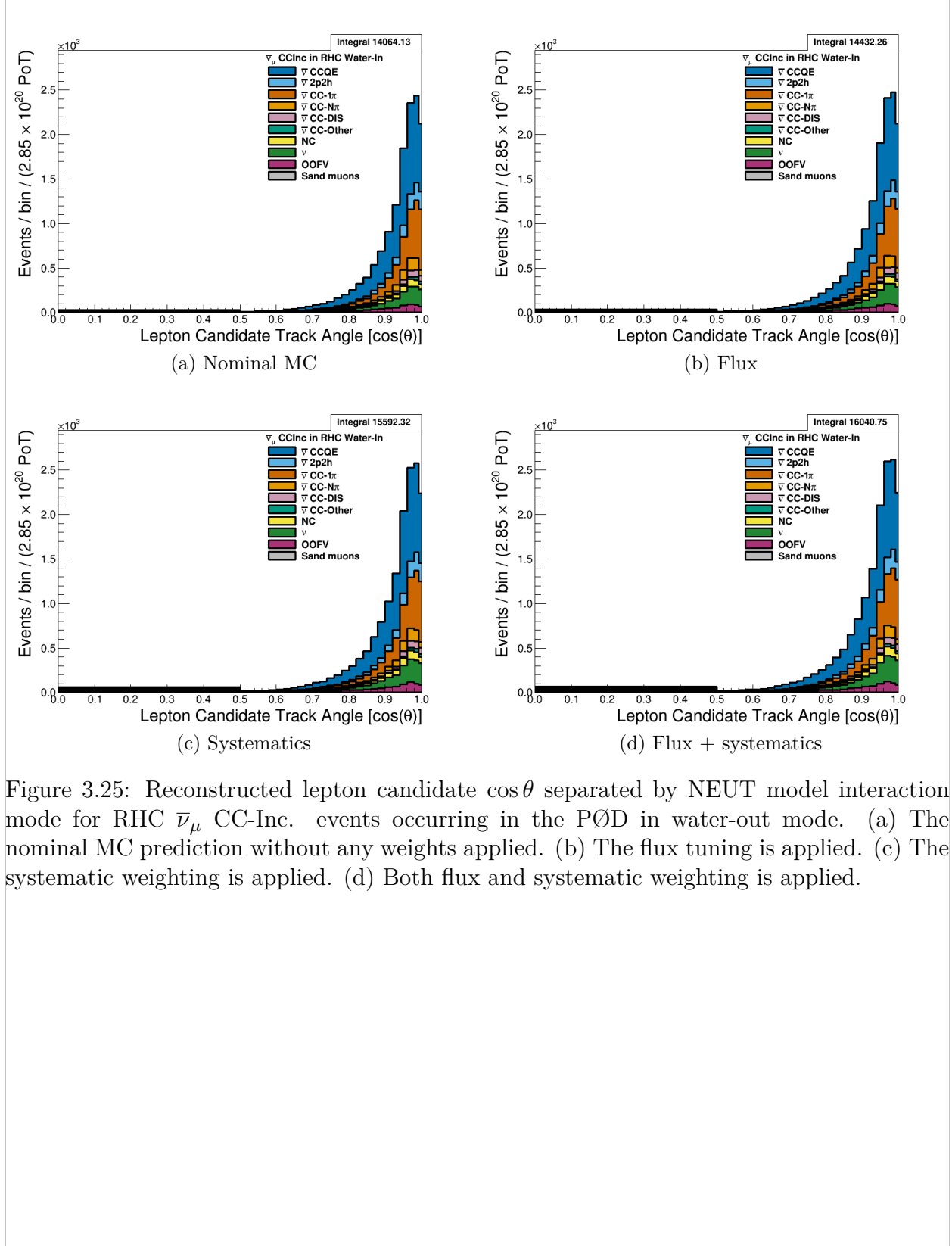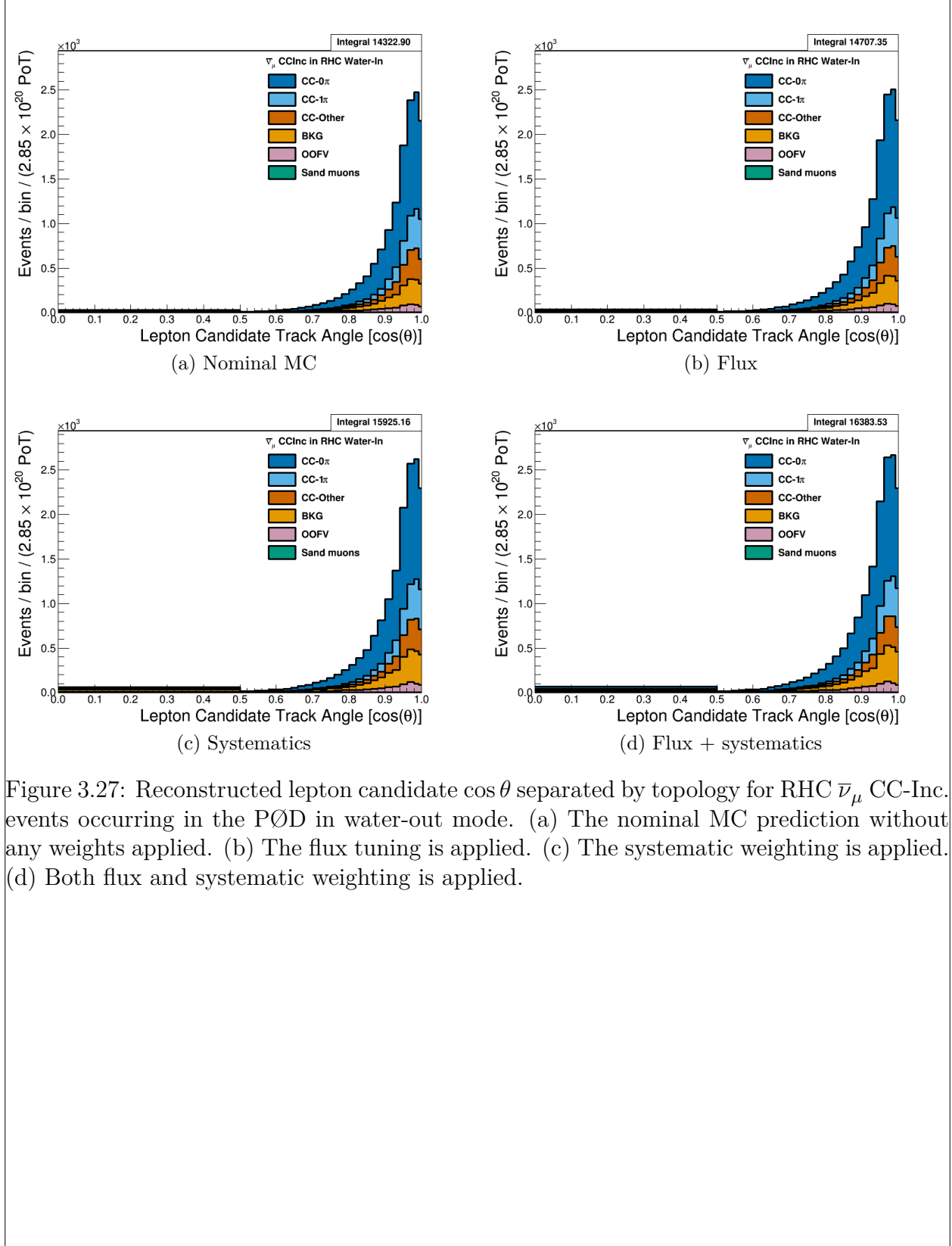
Figure 3.27: Reconstructed lepton candidate $\cos\theta$ separated by topology for RHC $\overline{\nu}_\mu$ CC-Inc. events occurring in the PØD in water-out mode. (a) The nominal MC prediction without any weights applied. (b) The flux tuning is applied. (c) The systematic weighting is applied. (d) Both flux and systematic weighting is applied.
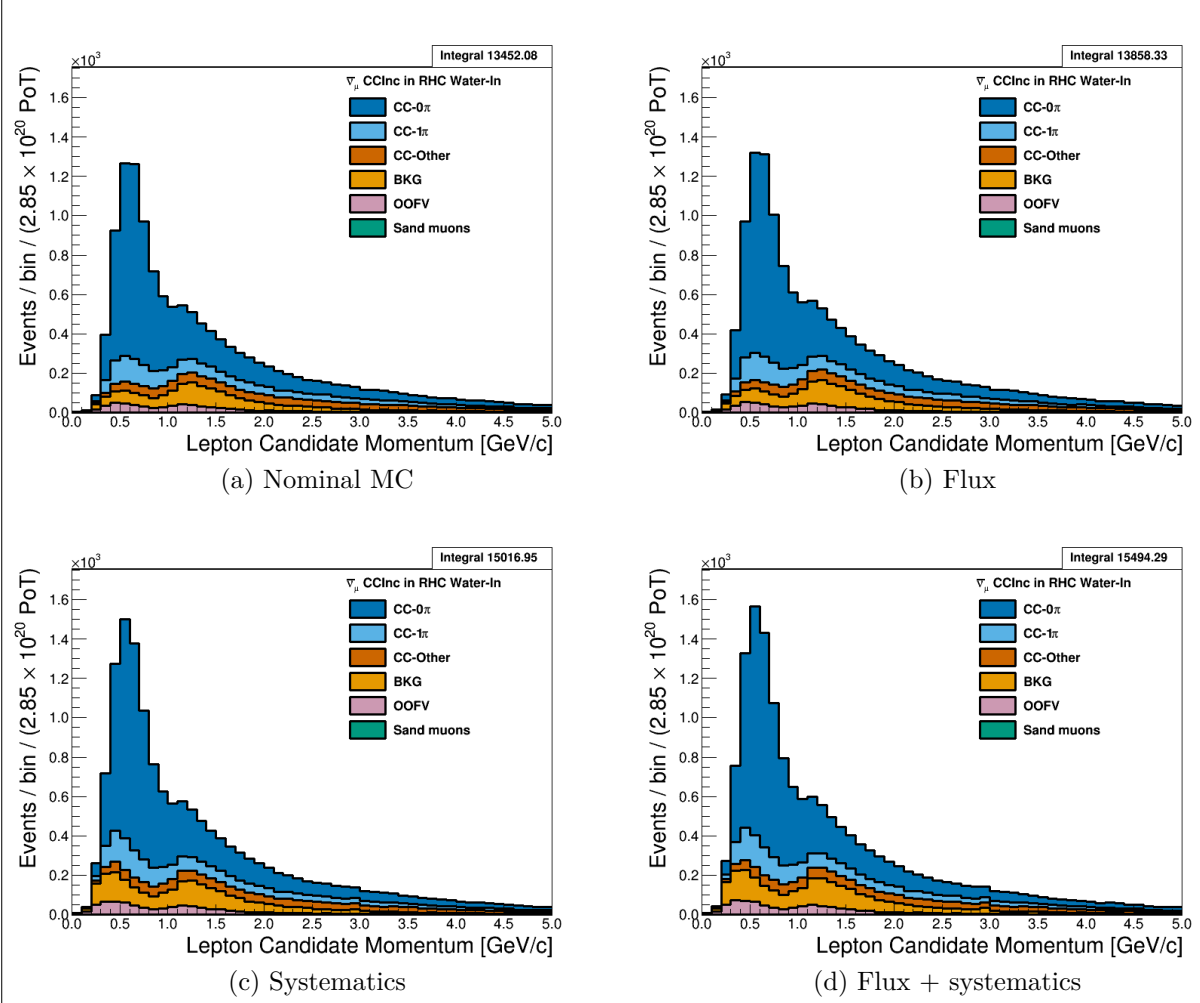
(a) Nominal MC

(b) Flux

(c) Systematics

(d) Flux + systematics

Figure 3.28: True neutrino energy associated with the lepton candidate separated by NEUT model interaction mode for RHC $\overline{\nu}_\mu$ CC-Inc. events occurring in the PØD in water-out mode. (a) The nominal MC prediction without any weights applied. (b) The flux tuning is applied. (c) The systematic weighting is applied. (d) Both flux and systematic weighting is applied.
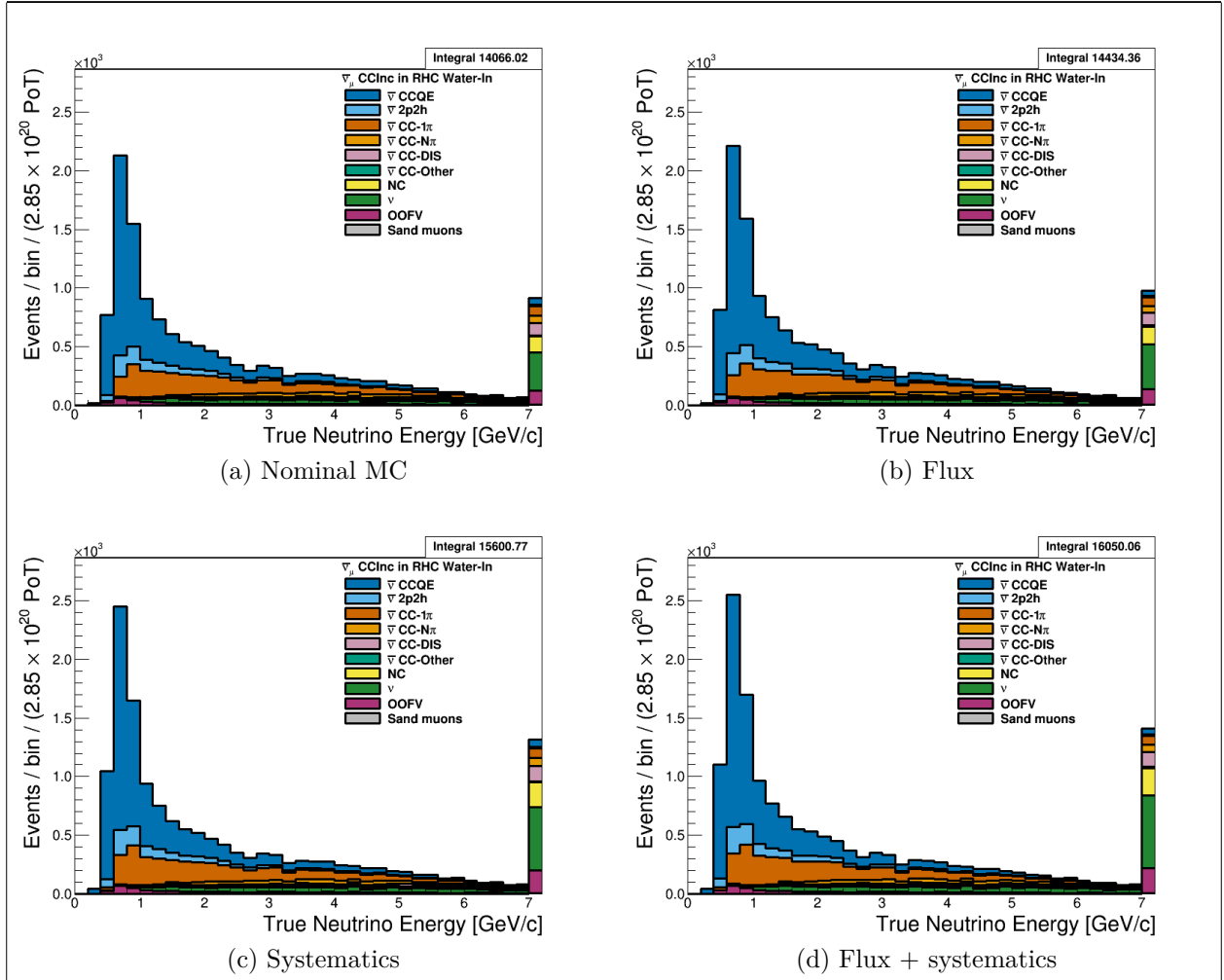
ν_μ RHC:Add figures here

3.5.2   CC-1 Track (CCQE Enhanced)

Add figures here

3.5.3   CC-N Tracks (CCnQE Enhanced)

3.5.4 Differences Between Water-Out and Water-In Samples

4 PØD-Only BANFF Parameterization

PØD-only BANFF

5 Fitter Validation

Fitter validation

6 Fitter Results

Fitter results

7 Discussion

Discussion

References

[1] S. Baker and R. D. Cousins. Clarification of the use of Chi-Square and Likelihood Functions in Fits to Histograms. *Nucl. Instrum. Meth.*, A221:437–442, 1983. 13

[2] S. Bienstock and Others. *Constraining the Flux and Cross Section Models with Data from the ND280 Detector using FGD1 and FGD2 for the 2017 Joint Oscillation Analysis*, August 2017. T2K-TN-324 v3. 17

[3] S. Bolognesi and Others. *NIWG model and uncertainties for 2017 oscillation analysis*, April 2017. T2K-TN-315 v5. 17

[4] T. Campbell. *Measurement of the ν_μ CC-0π Double Differential Cross Section on Water in the PØD*, February 2018. T2K-TN-328. 19

[5] T. Campbell and Others. *Analysis of ν_μ Charged Current Inclusive Events in the PØD in Runs 1+2+3+4*, Mar 2014. T2K-TN-80 v4. 19, 21, 22

[6] R. Das and Others. *Measurement of Induced Charged Current Cross Section on Water using the PØD and TPC*, November 2014. T2K-TN-100. 19

[7] K. Gilje. *Geometry and Mass of the π^0 Detector in the ND280 Basket*, Apr 2012. T2K-TN-73 v3.1. 22

[8] M. Hartz and Others. *Constraining the Flux and Cross Section Models with Data from the ND280 Detector for the 2014/15 Oscillation Analysis*, May 2015. T2K-TN-220 v4. 12, 13

[9] A. Hillairet and Others. *ND280 Reconstruction*, Nov 2011. T2K-TN-72 v1. 22

[10] T. Koga. *Comparison between BANFF post fit results and on-axis detectors*, 2017. 8

[11] K. Mahn and Others. *Implementation of new cross section parameters for the 2017 oscillation analysis*, 2017. T2K-TN-307. 17

[12] G. Wikström and A. Finch. *Global Kalman vertexing in ND280*, Feb 2018. T2K-TN-46 v3. 20

[13] T. Yuan and Others. *Double Differential Measurement of the Flux Averaged ν_μ CC0Pi Cross Section on Water*, Aug 2016. T2K-TN-258 v4.6.1. 19, 21

Nomenclature

BANFF The **b**eam **a**nd **n**ear detector task **f**orce is the group responsible for providing near detector constraints on cross section and flux model parameters.

CC-0π A **c**harged **c**urrent zero pion selection is an exclusive selection that selects neutrino interaction topologies only one MIP-like particle.

CC-Inclusive A **c**harged **c**urrent event selection that selects all neutrino interaction topologies with an outgoing charged lepton.

FD The **f**ar **d**etector refers to the particle detector in a long baseline neutrino oscillation experiment that is located far away from the neutrino production source where oscillated neutrinos are observed.

FGD A **f**ine **g**rain **d**etector is a detector made of closely spaced, small scintillating bars designed to provide precise resolution of charged particle tracks

FHC The **f**orward **h**orn **c**urrent beam configuration that focuses positively charged particles into the particle decay pipe. This configuration produces a very pure ν_μ neutrino beam

HMNT The **h**ighest **m**omentum **n**egatively-charged **t**rack in the bunch

HMPT The **h**ighest **m**omentum **p**ositively-charged **t**rack in the bunch

MIP A **m**inimum **i**onizing **p**article

ND280 The **N**ear **D**etector of T2K which is **280** meters away from the neutrino source.

ND The **n**ear **d**etector refers to the particle detector in a long baseline neutrino oscillation experiment that is located close to the neutrino production source before neutrino oscillations occur.

CECal The **C**entral **ECal** detector which is a part of the PØD inside ND280

PØD The π^0 detector (**pi-Ø d**etector)

PØDule A collection of two active scintillator bar layers inside the PØD

RHC The **r**everse **h**orn **c**urrent beam configuration that focuses negatively charged particles into the particle decay pipe. This configuration produces a $\overline{\nu}_\mu$ enriched neutrino beam with a significant ν_μ contribution.

FV The **f**iducial **v**olume of a detector is the region where the detector response is well understood

TPC A **t**ime **p**rojection **c**hamber is a device that detects and tracks charged particles with the application of strong electric fields

Tracker The region of ND280 consisting of two FGDs and TPCs

Global The Global reconstruction module responsible for making joined tracks between the subdetectors inside ND280

USECal The **U**p**s**tream **ECal** which is a part of the PØD inside ND280